Electron microscopy / Microscopie électronique

Using electron beams to investigate carbonaceous materials

Apports de la microscopie électronique à l'étude des matériaux carbonés

Clemens Mangler, Jannik C. Meyer *

University of Vienna, Department of Physics, Boltzmanngasse 5, A-1090 Wien, Austria

A R T I C L E I N F O	A B S T R A C T
Article history: Available online 23 January 2014 *Keywords:* Carbon Carbon nanotube Graphene High-resolution electron microscopy *Mots-clés :* Carbone Nanotube de carbone Graphène Microscopie électronique à haute résolution	This paper provides a brief review on electron microscopic studies of carbon materials. We discuss all aspects ranging from sample preparation via basics of the structure and its reciprocal space representation to high-resolution imaging and spectroscopy. Emphasis is given to recent developments, namely aberration-corrected electron microscopy and the newest low-dimensional carbon allotrope, graphene. © 2013 Académie des sciences. Published by Elsevier Masson SAS. All rights reserved. R É S U M É Cet article présente une brève revue des études réalisées en microscopie électronique sur des matériaux carbonés. Tous les aspects essentiels y sont abordés, depuis la préparation des échantillons jusqu'à l'imagerie et la spectroscopie à très haute résolution spatiale, en passant par les mesures conventionnelles de structure dans l'espace réel et dans l'espace réciproque. Un intérêt plus spécifique est cependant consacré aux développements les plus récents, incluant, d'une part, l'outil, à savoir la microscopie électronique à correction d'aberrations, et, d'autre part, l'objet d'étude le plus étudié aujourd'hui, à savoir la variété allotropique de basse dimension, le graphène. © 2013 Académie des sciences. Published by Elsevier Masson SAS. All rights reserved.

1. Introduction

Electron microscopy (EM) and carbon materials have a long, fruitful, and highly versatile relationship. Carbon structures have been the subject of investigation already in very early studies [1–7], and still today, are among the most exciting topics. Carbon also serves as the probably most widely used support films, and it is often a nuisance as a vacuum contamination. Indeed, it is probably difficult to be engaged in electron microscopy without coming across carbon in one way or the other. Carbon materials are of particular interest for electron microscopic studies due to their immensely rich variety of shapes, allotropes, geometries and bonding configurations. The allotropes are commonly given as the bulk forms graphite and diamond, plus the nano-scale forms of nanotubes [8–10], graphene [11], and fullerenes [12]. These, in turn, can display further variations such as single-shell or multi-shell tubes. At the atomic level, the bonding configuration may deviate from the basic hexagonal shape, for example at defects, grain boundaries, or edges. This leads to a further variety of the shapes including carbon whiskers, fibers, cones [13], platelets, ribbons [14,15], onions [16,17], scrolls [18], and many others. Moreover, exotic forms of carbon such as single-atomic carbon chains have been observed by high-resolution transmission electron microscopy (HRTEM) [19–21].

---

* Corresponding author.
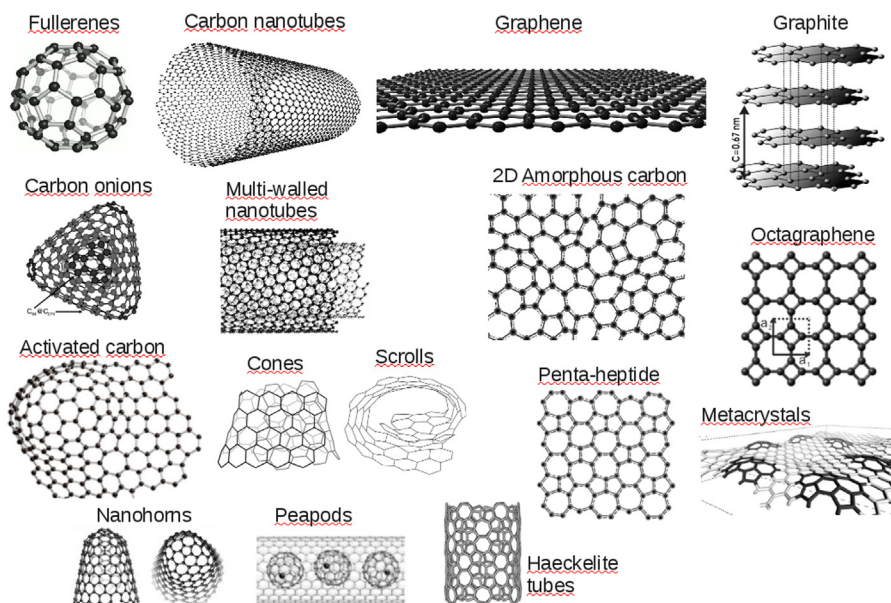 *E-mail address:* jannik.meyer@univie.ac.at (J.C. Meyer).

Fig. 1. A selection from the large variety of sp^2-bonded carbon forms. At the top, the archetypal shapes for an allotrope of each dimensionality (0D to 3D) are shown, namely fullerenes, carbon nanotubes, graphene, and graphite. However, a virtually unlimited number of sp^2 bonded carbon forms can be generated by the introduction of non-hexagonal rings, curvature, stacking, or encapsulation. Examples include carbon onions [32], multi-walled nanotubes [9,33], 2D amorphous carbon [34], activated carbon [35], cones and scrolls [13], nanohorns [33] or peapods (fullerenes encapsulated in carbon nanotubes) [33]. The non-hexagonal crystalline forms, such as pentaheptide [36], octagraphene [37] or haeckelite metacrystals [38] and tubes [39], have not been experimentally observed so far. Some of the images are reprinted with permission from Refs. [13,32,33,35,37,39], and are copyright 2002, 2004, 2006, 2008 Elsevier (Refs. [13,32,33,35], 2012 AIP Publishing LLC (Ref. [37]), and copyright 2000 by the American Physical Society (Ref. [39]).

Carbon materials represent a particular challenge for TEM imaging due to the low intrinsic contrast and high susceptibility to radiation damage. The low-dimensional forms (graphene and carbon nanotubes), typically only contain one or a few atoms in the projection of a high-resolution TEM or Scanning-TEM (STEM) image. Therefore, structures and defects in fullerenes, carbon nanotubes, and graphene layers require special care for a detailed analysis. Nevertheless, most of the low-dimensional carbon allotropes have been discovered or identified from electron microscopic studies. The earliest descriptions of tubular carbons date back to 1952 [1], while the widespread interest into carbon nanotubes was initiated by the electron microscopy work of Iijima in 1991 [9]. Single-layer pieces of graphite were described as early as 1962 based on TEM observations [7]. Some of the less regular shapes, such as carbon onions or cones, often appear as by-product during carbon nanotube synthesis and are subsequently found during TEM characterization of the material [22].

Besides being the sample or sample support, thin carbon films have been used as phase plates [23] or foil lenses [24,25]. The specific geometries of some nano-carbon materials, especially the nearly one-dimensional shape of carbon nanotubes and the high curvature at their tips, may lead to further applications as electron optical elements. Carbon nanotubes can serve as excellent field emitters [26–28] due to the high-field enhancement at their tips, with possible applications in displays, X-ray sources or electron microscopes [29]. Moreover, they can serve as nano-scale bi-prisms [30], and focusing elements [31].

2. The zoo of carbonaceous materials

Carbon is one of the most versatile elements in that it can form an enormous range of structures and compounds. Chemistry classes are typically split into organic chemistry—everything related to carbon—and inorganic chemistry: everything else. No other element gathers that much attention. Here, we even consider just a tiny subsection of organic compounds, namely those made purely from carbon and exhibiting sp^2 type bonding. This by itself is sufficient to fill a chapter or a book.

Studies of the sp^2 bonded forms of carbon make up the predominant part among HRTEM and STEM investigations of carbonaceous materials. The nano-scale and low-dimensional forms, such as carbon nanotubes, graphene sheets, fullerenes, carbon cones, scrolls, and similar types, are rather similar in their microscopic analysis (contrast, radiation damage, etc.) due to the same underlying sp^2 bonded network. Graphene may be considered as the most elementary form of sp^2 bonded carbon, and hence, insights to graphene can be beneficial also to the understanding of related structures. The sp^3 bonded form of carbon, diamond, is (from a microscopy perspective) rather similar to typical bulk crystalline materials, and will not be further discussed in this article.

Fig. 1 is a brief, and inevitably incomplete, illustration of the wide variety of materials that can be generated from sp^2 bonded carbon. In all these materials, the carbon atoms are bonded to three neighbors in a planar or nearly planar geometry. The differences are only the local topology (number of atoms in a ring) and the global topology, i.e. the flat or curved shapes of graphene layers or tubes. In addition, the material may be assembled into layers or concentric shells.
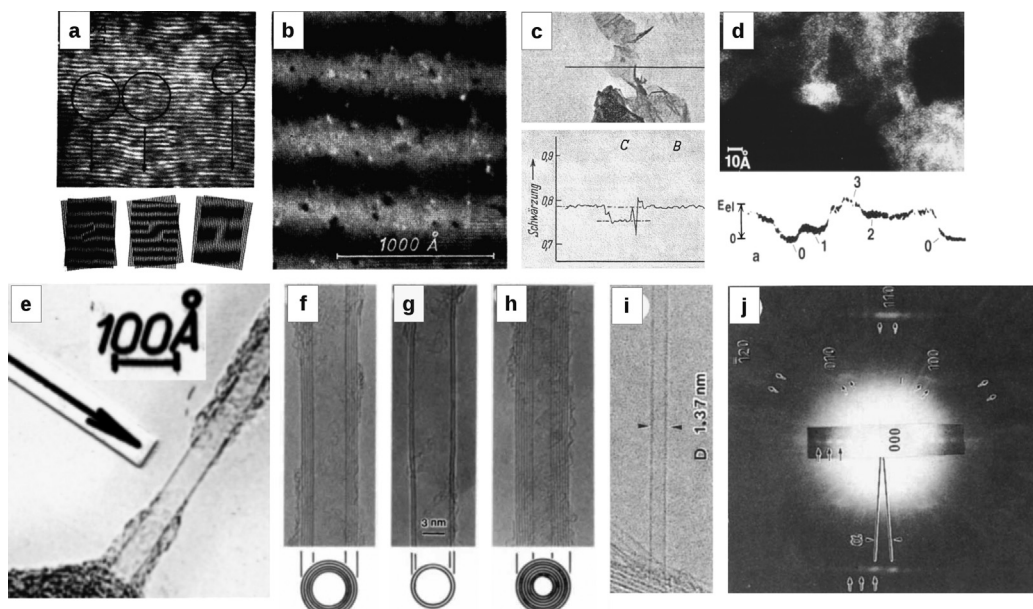
Fig. 2. Early images of graphitic carbon and nano-carbon structures. (a+b) Moiree patterns revealing dislocations (a) and point defects (b) in graphite [4,5,40] (1961). (c) A study of ultra-thin graphite, claiming mono-layer thickness on the basis of intensity variations (1962) [7]. (d) ADF–STEM observation of discrete intensity steps in thin carbon samples (1970) [41–43], may indicate the presence of mono-layers. (e) Endo's early image of a carbon nanotube (1976) [44], (f–i) Multi-walled and single-walled carbon nanotubes as presented by Iijima (1991, 1993) [8,9]. (j) The electron diffraction pattern unambiguously identifies the atomic structure of a hexagonal lattice wrapped into a cylinder [8]. Figures reprinted with permission from Refs. [4,7–9,40,42,44]; Copyright 1961 AIP Publishing LLC (a), (1961) Elsevier (b), (1962) The Bunsen Society for Physical Chemistry (c), (2012) Elsevier (d), (1976) Elsevier (e), (1991) and (1993) Nature Publishing Group (f–j).

Graphite was among the first materials where defects in the lattice structure, in particular dislocations, could be characterized by electron microscopy [4,5,40]. Already at that time, ultra-thin graphite was prepared by mechanical exfoliation. The Moiree pattern that appears with the (frequently occurring) misstacked layers of graphite is very sensitive to tiny distortions in the crystal structure. Hence, it was easily possible to detect a variety of defects even though the instrumental resolution in these early works was far from atomic dimensions.

Fig. 2 shows a short overview of historical electron microscopic images of carbon structures. Both tubular [1] and planar forms of graphitic carbon have been around since the 1950s–1960s, but the sample preparation and imaging performance have seen tremendous advances since then. While, for example, the (presumably) single-walled carbon nanotube in M. Endo's work [44] (Fig. 2(e)) was likely an exception in a material dominated by multi-shell tubes and fibers, the catalytic growth developed later on permitted the synthesis of sizable amounts of extended single-shell carbon nanotubes. Moreover, the electron diffraction analysis revealed the well crystallized lattice of the nanotube [8] as a seamless cylinder of a hexagonal network. Similarly, some early descriptions of ultra-thin graphitic layers (Fig. 2(c), (d), [7,41]) indicate the presence of mono-layers, but the interpretation is debatable.

3. Sample preparation

One of the most important aspects of any successful EM analysis is the preparation of an adequate sample. This is even more significant for TEM, since—as the name implies—TEM requires that the electrons are transmitted through the sample and can reach the detector without any substantial interfering contributions from the sample support or any surface layers of remains of the sample preparation process. For carbonaceous samples such as graphene or carbon nanotubes, any support film or thick surface layer would produce a stronger contrast in the direct image than the thin and light elements of the material itself. The usual approach to mitigate this effects is a careful preparation of free-standing samples.

3.1. Carbon nanotubes

Synthesis of carbon nanotubes can be achieved by a multitude of different methods (see, e.g., Ref. [45] for a review), and there is a similarly large variety of ways to obtain free-standing nanotubes that would be suited for a TEM analysis. One widely used approach for the transfer of carbon nanotubes to a TEM grid consists of mechanical scraping of the grown tubes followed by dispersion in a solution agent. Mixing of the dispersion of the tubes is often facilitated by ultrasonic agitation [46]. Subsequently the solution containing the dispersed nanotubes is dropped onto a TEM grid followed by a drying procedure. This approach is easy and simple; however, it has several drawbacks for the study of the nanotubes by electron microscopy. One problem is that carbon nanotubes (especially single-walled tubes) have a strong tendency to form

bundles when deposited from a solution, and high-resolution images of bundles are much more difficult to interpret than images of isolated tubes. One might spend a significant portion of the time searching for isolated nanotubes within a sample that is dominated by thicker bundles. On top of this, for an analysis of the nanotubes by electron diffraction, one has to find sections where the tubes are straight within the area that is used to form a diffraction pattern.

A variety of specialty techniques have been developed in order to obtain well-defined isolated single nanotubes in a TEM-compatible free-standing geometry, usually integrated into nanostructured devices that allow a simultaneous measurement of electric, optical or mechanical properties [47–54]. Using in-situ TEM, it was achieved to directly monitor the growth of carbon nanotubes [55–57]. Another technique involves embedding the grown nanotubes in an epoxy resin followed by cutting using a diamond ultramicrotome [58] or by thinning using focused ion beam (FIB) [59]. These methods can provide cross-sectional views of the carbon nanotubes.

3.2. Graphene

Grinding of graphite and dispersion of the result onto a carbon grid is a well-known approach to make thin graphitic test samples for electron microscopy. However, this method can only provide tiny pieces of graphene, typically at edges of thicker crystals. The preparation of extended suspended graphene layers, starting from exfoliated sheets or CVD-grown graphene, is still a challenge. However, in the past few years, extended graphene membranes on TEM grids have become available as commercial products.

Early extended (few micron size) graphene samples were produced by exfoliation of graphite, where thin layers are produced by repeated peeling of bulk graphitic pieces using a scotch tape followed by a transfer to a Si/SiO$_2$ chip (the thin films can be seen there, because of the additional optical path shifting the interference colors; for details see Refs. [11,60]). After identification of potential mono-layer sheets by optical microscopy, they need to be transferred onto a free-standing grid. In the first successful approach, a metal scaffold was prepared on top of the graphene sheet by electron beam lithography and the underlying substrate was subsequently removed [61,62]. This approach was later improved to obtain single-crystalline mono-layer free-standing membranes with up to 25 μm in diameter [63]—much more than what is needed for electron microscopic studies, but enabling a demonstration of optical properties in the transmission geometry [64]. A simple transfer of mechanically exfoliated graphene sheets to standard commercially available TEM grids was developed later [65]. Graphene sheets that are prepared via oxidation (graphene oxide, GO), and the reduced form (reduced graphene oxide, RGO) may be fished out of a solution, using standard TEM grids [66–68]. However, for preparation of the solution as well as deposition onto the grid, parameters have to be carefully controlled in order to obtain single layers in a reasonable fraction of the area, rather than thick stacks of sheets or nearly empty grids.

During the chemical vapor deposition (CVD) synthesis, thin films of carbon are grown on metal substrates by a surface-catalyzed process [69–71]. These large-area samples can be transferred to TEM grids, by coating with a sacrificial support film, removal of the metal, deposition onto the grid and finally removal of the sacrificial layer. Examples of such a transfer process as well as resulting images are given in Refs. [72–76]. The study in Ref. [75] even adds a marker system in the process, so as to find the same position in HRTEM and Raman investigations. While almost all studies have used graphene membranes in a top view, cross-sectional imaging can reveal stacking of layers or presence and absence of contamination in-between the layers [77], and does not require free-standing membranes.

4. SEM

Scanning electron microscopy (SEM) is an invaluable tool to verify sample preparation or the integration of the material into a nanofabricated device. By SEM, it is possible to observe structures that are not accessible by TEM, for example objects on a substrate. Fig. 3 shows examples of SEM images for graphene on a metallic and insulating substrate [73], carbon nanotubes on a substrate [78], as well as an individual MWCNT integrated into a tensile testing setup [79]. Due to the high electron transparency of graphene, the contrast (e.g., layer thickness) strongly depends on the underlying substrate (Fig. 3(a), (b)). For carbon nanotubes on an insulating substrate, the contrast in the SEM can be strongly influenced by charging of the tubes under the beam, especially at low voltages [80]. This effect is actually beneficial as it increases the visibility of the tubes (Fig. 3(c)).

5. Effects of electron irradiation

5.1. Radiation damage

One of the most important issues regarding electron microscopy of carbonaceous materials, and low-dimensional materials in general, is their stability under the electron beam. Being a light element, carbon is more easily ejected from its lattice position. At the same time, it produces only a small contrast so that higher doses are needed in order to obtain a sufficient signal to noise ratio.

A number of mechanisms of radiation damage are known, which include knock-on damage, ionization damage, beam-induced etching, and heating. The damage that occurs in sp^2-bonded carbon structures appears to be dominated by knock-on
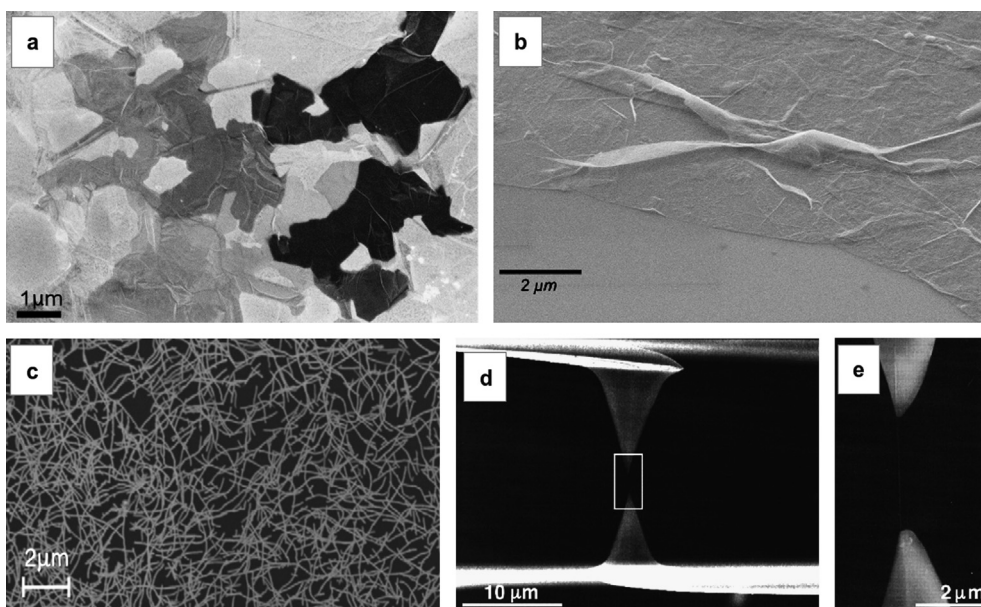
Fig. 3. SEM micrographs of graphene and carbon nanotubes. (a) Secondary-electron image of few-layer graphene on a nickel surface, showing a clear thickness (layer number) contrast. Empty areas (bare Ni surface) can be ruled out, since even in the thinnest areas, fold and creases can be discerned [73]. (b) SEM image of the same few-layer graphene sample after transfer from Ni to a silicon/silicon dioxide substrate. (c) A network of single-walled carbon nanotubes grown directly on a silicon/silicon dioxide substrate [78]. (d+e) An individual carbon nanotube attached to two cantilever tips for the purpose of tensile testing [79]. (a+b) reprinted with permission from Ref. [73], Copyright 2010 Elsevier; (c) reprinted with permission from Ref. [78], Copyright 2007 Elsevier. (d+e) reprinted with permission from Ref. [79], Copyright 2000 The American Association for the Advancement of Science.
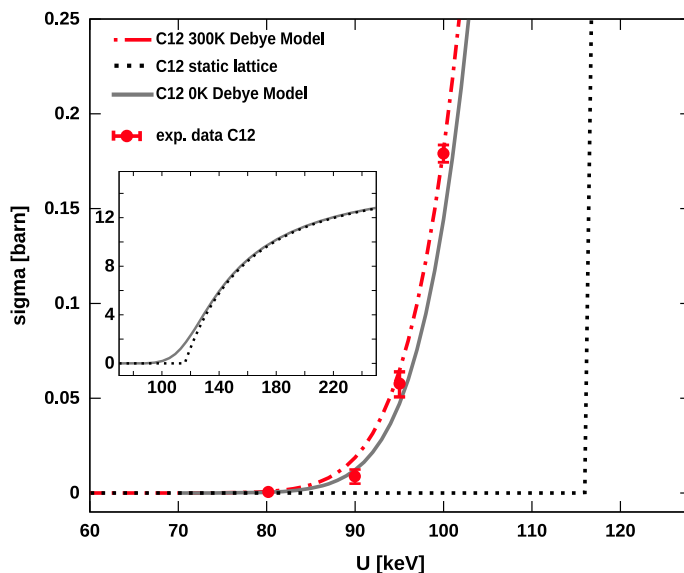

Fig. 4. (Color online.) Experimental and calculated sputtering cross sections for carbon atoms in a graphene sheet [89]. A good agreement is obtained only if the lattice vibrations of the material are taken into account in the calculation.

damage [81–90], while chemical etching also plays an important role [87,89,91]. Chemical etching refers to a beam-activated process that involves oxygen or water in the column, and possibly contamination on the sample.

In the early days of electron microscopy, the commonly used route to increase the resolution was by increasing the acceleration voltage and thus decreasing the electrons wavelength. But it was only after the emergence of the first correctors that this paradigm shifted. The increase in performance of modern corrected electron microscopes allows a decrease in acceleration voltage without sacrificing resolution. Indeed, the demand to investigate carbon materials was a significant part of the motivation for several recent microscopic developments towards reduced operating voltages [92–94]. Carbon atoms within a pristine graphene lattice indeed are remarkably stable under electron irradiation of 80 kV (Fig. 4). However, defects are still modified under an 80-kV beam (i.e., they transform from one type of defect into another) [95]. Objects such as

fullerenes or graphene edges clearly benefit in terms of stability from substantial further reduction of the electron energy, e.g. to 20–30 kV [93,96].

5.2. Beam-induced material modifications

If the effect of the electron beam on the material is sufficiently predictable and controllable, one can make use of it in order to structure or otherwise modify the sample. The most straightforward way to do this is to make use of the knock-on displacement effect in order to create atomic vacancies [97–99] or extended holes [100]. However, it is important to consider the (temperature-dependent) structural reorganization of the material in response to such modifications [101, 102]. In particular, mobile carbon atoms can re-fill vacancies at rates that noticeably slow down the cutting of a carbon nanotube [103], and at elevated temperatures, graphene re-organizes itself fast enough to display a pristine lattice even under 300-kV irradiation [102]. At very low voltages, such as those available in a scanning electron microscope (SEM), cutting of carbon materials can be achieved via the chemical etching effect: in Ref. [91], water vapor was intentionally added to the column in order to increase the speed of cutting multi-walled carbon nanotubes. Besides cutting, it is possible to deposit carbon onto graphene under a focused electron beam [65], an approach that is also known as contamination lithography.

6. Diffraction-based methods

On the theoretical side, the understanding of TEM images and electron diffraction patterns of graphene, carbon nano-tubes, and related materials is relatively simple. With a thickness of only one or a few carbon atoms in the projection along the electron beam, the interaction between the beam and the sample can be approximated as a weak perturbation in the phase of the electron wave given by the electrostatic potential of the sample. Indeed, these materials are probably the only ones where it is reasonable to use a weak phase object approximation when studied at typical electron energies at or above 60 kV (at 20 kV, even graphene is a strongly scattering object [104]). The single-slice approximation is reasonable for a single layer of atoms (and as a first approximation for few-layer samples), but must be replaced by multi-slice calculations for thicker samples. Indeed, already for a thickness of two layers, a deviation from the simple projection model has been detected [105].

We briefly consider the intensities that are observed in an electron diffraction pattern of single-walled carbon nanotubes or single- and double-layer graphene sheets. For a quasi-one-dimensional object, such as a carbon nanotube (Fig. 5(a)), we find non-zero intensities on extended discs in reciprocal space (Fig. 5(b)). The Ewald sphere cuts trough these discs and hence we find extended lines in the electron diffraction pattern (Fig. 5(c)). The positions of these lines can be constructed by considering the carbon nanotube as a set of helices, similar to DNA [106,107]. Other constructions based on a hexagonal lattice curved into a cylinder are possible [108–110]. For details of the carbon nanotube diffraction pattern, the reader is referred to the extensive literature [53,106–109,111–114]. Accurate measurements of the peak positions allow one to determine not only the nanotube indices, but also elliptical deformation [115], inclination toward the electron beam [53], or torsional deformation [51,116], which was also demonstrated experimentally [51].

For graphene, a two-dimensional structure, we find non-zero intensities on infinite rods extended along the direction orthogonal to the sample plane (in crystallography terms, the zero-order Laue zone is infinitely large). This is illustrated in Fig. 5(d), where the intensities in reciprocal space are again rendered in a 3D perspective view. The blue plane now represents a diffraction pattern that would be obtained under normal incidence. Fig. 5(e) shows the primary lattice spacings drawn onto a real-space image. These distances may also serve as a scale reference in TEM or STEM images of graphene. Note that there is no Bragg reflection that corresponds to the nearest-neighbor atomic distance in graphene (1.42 Å) or to the hexagon center separation (2.46 Å). Fig. 5(f)–(h) shows experimental electron diffraction patterns of mono-layer, AB-stacked bi-layer and turbostratic bi-layer graphene, respectively. For mono-layer graphene, a unique situation occurs: the first and second sets of reflections are of nearly identical intensities (Fig. 5(f), see also Fig. 6(c)). For AB-stacked multi-layer graphene, the second set of peaks is always significantly stronger than the first hexagon (Fig. 5(g)). Finally, the turbostratic case is easy to identify from multiple sets of hexagons (Fig. 5(h)).

Fig. 6(b), (c) shows the elementary structural properties of graphene in reciprocal space. Fig. 6(b) shows structure factors alone, and Fig. 6(c) multiplied with the atomic form factor for carbon (i.e. Fig. 6(c) is a simulated electron diffraction pattern based on the independent-atom model, IAM). The intensities are normalized to the first set of reflections. It has to be considered as a coincidence that the intensity ratio of the first and second set of peaks in the graphene diffraction pattern is close to 1. Indeed, while the standard simulation based on the IAM predicts a ratio of 0.9, the DFT-based ratio is 1.05 (DFT-based potentials were calculated within the work of Ref. [117]), which is closer to the experimental values from well crystallized graphene.

The larger-scale crystal structure of graphene samples nicely lends itself to an analysis by dark-field TEM. By this method, which is relatively simple and can be carried out on almost any TEM, it is possible to map the distribution of grains in a poly-crystalline sample [76,118], study the stacking order and stacking faults in few-layer graphene [119], and corrugations [61,120]. Such dark-field maps can be recorded even if the graphene is placed on a thin support membrane, which has opened the door to correlated studies of grain structure and electronic properties [121].
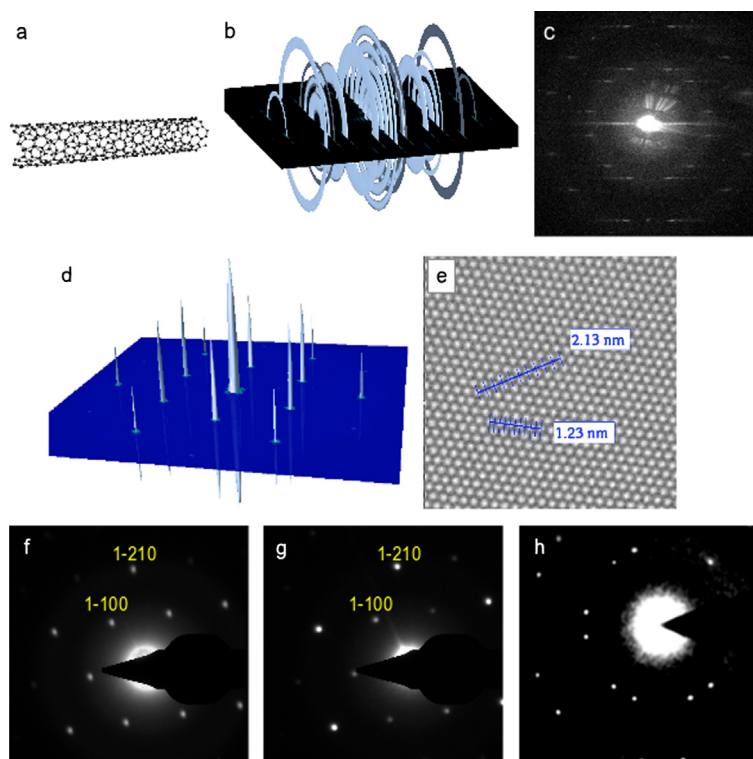
Fig. 5. (Color online.) Real and reciprocal space representations of carbon nanotubes and graphene. (a) Atomistic model of a SWCNT, and (b) 3D Fourier transform of the structure. Blue discs indicate non-zero intensities in reciprocal space. (c) Experimental electron diffraction pattern of a single-walled carbon nanotube [53]. (d) Reciprocal space representation of graphene. Non-zero intensities are present on continuous rods normal to the plane. (e) Real-space distances corresponding to the first two sets of Bragg reflections. Shown here is $10\times$ the respective distance of 2.13 Å or 1.23 Å. (f–h) Experimental electron diffraction of mono-layer graphene, AB-stacked bi-layer graphene, and turbostratic bi-layer graphene, respectively.

7. High-resolution imaging

Due to the timing of the material discoveries and instrumental developments, the vast majority of electron microscopic studies on carbon nanotubes so far were carried out with conventional (uncorrected) transmission electron microscopes, while the advent of graphene coincided with the more widespread use of aberration-corrected imaging. For uncorrected HRTEM imaging of low-dimensional graphitic materials, one usually has to make a compromise in the electron energy, to be high enough to resolve the layer spacing or even the graphene lattice while being low enough to briefly maintain a stable sample. Only few workers achieved to resolve the hexagonal lattice in single-walled carbon nanotubes without aberration correction [112,122,123].

The successful correction of electron optical aberrations [124,125] enabled lattice-resolution transmission electron microscopy at electron energies near or below the knock-on threshold of sp^2-bonded carbon structures [126–128]. As already mentioned, the demand to investigate carbon materials was a significant part of the motivation for several recent microscopic developments, in particular towards reduced operating voltages [92–94]. In addition, the absence of delocalization in the aberration-corrected image enables an unambiguous identification of defect structures [34,128,129], dislocations [66, 128,130,131], grain boundaries [76,118], substitutional doping [117,132,133], and even amorphous configurations [34,66] (Figs. 6–8).

Aberration-corrected transmission electron microscopy or scanning transmission electron microscopy can provide information about these materials that are not easily accessible by other means. For example, the non-hexagonal rings are difficult to distinguish by spectroscopic methods, since the local bonding geometry is rather similar to the hexagonal lattice. Also, the curved surfaces of some of the allotropes are difficult to access with scanning probe instruments. The local topology, i.e. the number of carbon atoms in a ring, is a rather important measure in nano-carbon structures: Pure topological defects are (by definition) a deviation from the hexagonal lattice without added or missing atoms, with the Stone–Wales (SW) defect [135] being the most simple example. Vacancies and multi-vacancies typically reconstruct into configurations that involve non-hexagonal rings [34,136]. Dislocation cores incorporate an unpaired pentagon–heptagon configuration [66,123,137] and grain boundaries in graphene display an arrangement of pentagons and heptagons that patch the mismatch between the lattice orientations [76,118]. Identification of these configurations is therefore pivotal to understanding sp^2-bonded carbons.
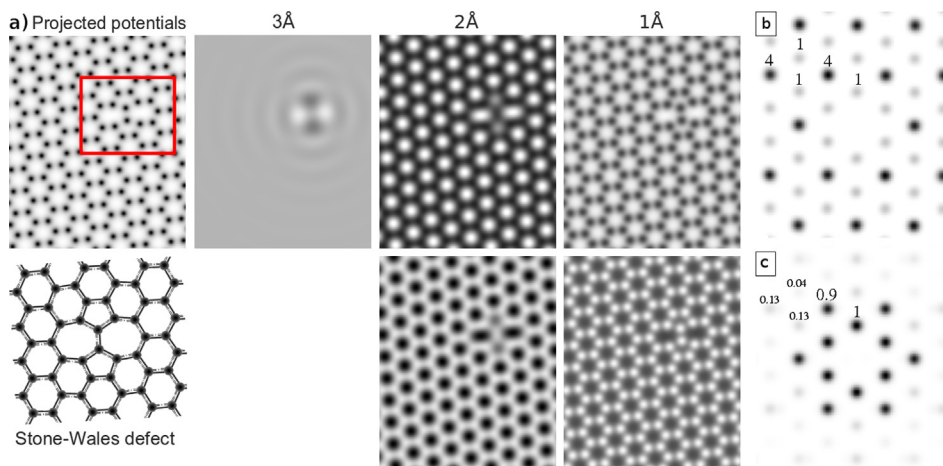
Fig. 6. (Color online.) (a) A graphene sheet with a Stone–Wales defect (red box) at different spatial resolutions. The upper left image shows the projected potentials (infinite resolution), with dark contrast representing higher projected potentials. The lower left image shows the atomistic model of the Stone–Wales defect in graphene [134]. Other images show the projected potentials limited to 3 Å, 2 Å and 1 Å resolution, with dark-atom (top) and bright-atom (bottom) conditions. (b) Structure factors of the single-layer graphene lattice. (c) Structure factors multiplied with the atomic form factor of carbon (i.e., simulated intensities in a diffraction pattern).
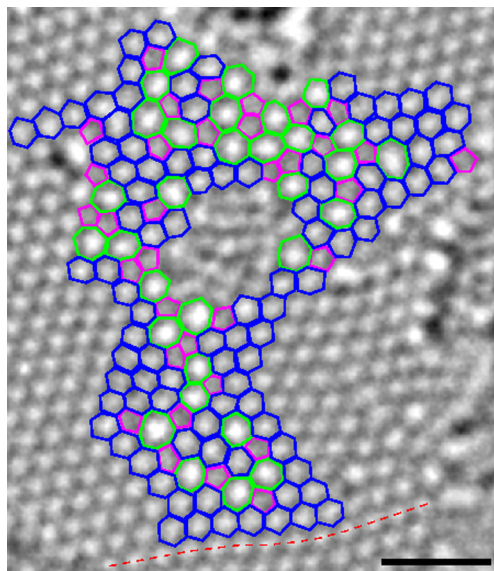

Fig. 7. (Color online.) Structural defect in reduced graphene oxide [66]. Shown are hexagons (blue), pentagons (pink) and heptagons or higher-ordered carbon rings (green). Red dashed line indicates a distortion in the lattice. Scale bar: 1 nm. For interpretation of references to color, see the online version of this article.

Fig. 6(a) shows how pentagon–heptagon configurations appear at different resolution. With ca. 3-Å resolution (uncorrected microscope at 80–100 kV), it is possible to detect even very low contrast defects against the featureless background of the pristine lattice, but an identification is difficult. At ∼2-Å resolution (lattice resolution is 2.13 Å for the graphene [10–10] reflection), the graphene hexagon centers are visible as dark or bright spots (depending on the imaging conditions). Here, a pentagon and heptagon can be identified, from having less respectively more contrast at its center as compared to the hexagon. At ∼1-Å resolution (1.08 Å for the graphene [20–20] reflection and 1.23 Å for the graphene [11–20] reflection), all atoms are separated. It is important to note that in principle a resolution of 2.13 Å is sufficient to identify all the different carbon ring topologies. Hence, with regard to the current developments towards low-voltage microscopy, it will be interesting to see which will be the lowest voltage where a resolution of 2 Å is achieved.

A real materials example where non-hexagonal configurations appeared as a surprise was the case of reduced graphene oxide (Fig. 7) [66]. Although this material had been extensively studied by spectroscopic means, the large extent of topological defects created by the oxidation–reduction procedure had not been described prior to our electron microscopic study. A different example, a gradual transformation from crystalline, hexagonal graphene to a completely amorphous structure made up from a seemingly random combination of pentagons, hexagons, heptagons and octagons was described in Ref. [34]
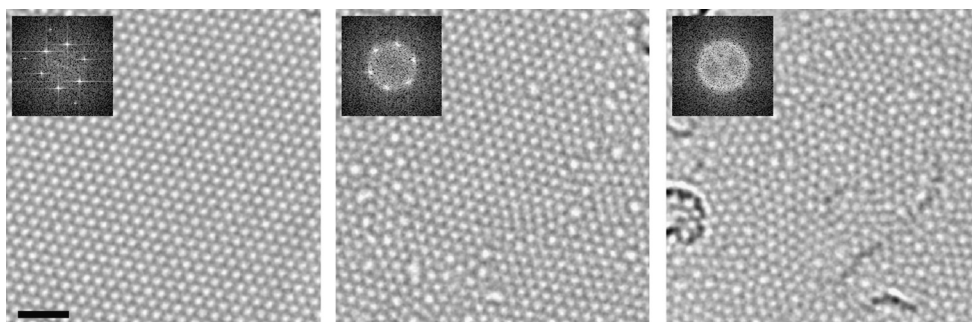
Fig. 8. Transformation from graphene to two-dimensional amorphous carbon under 100-kV electron irradiation (Ref. [34]). Scale bar: 1 nm.

and is shown in Fig. 8. Here, the transformation is driven by the electron beam: at energies close to the knock-on threshold, the predominant effect of the electron beam are bond rotations rather than atom removal, as also confirmed by molecular dynamics simulations [95].

Cs-corrected HRTEM images at 80 kV, such as shown in Fig. 7, or 100 kV in Fig. 8, are resolution-limited by chromatic aberrations and the energy spread of the source. The appearance and resolution correspond approximately to the 2 Å case of Fig. 6. By using a monochromator, resolution can be further increased [130,138], so that the second set of reflections (at 1.23 Å) becomes clearly visible. Aberration-corrected ADF–STEM images also clearly show the 1.23 Å and 1.08 Å reflections [94,133,139–141]. It might be somewhat easier to achieve this high resolution in the incoherent STEM image. Besides the differences between coherent and incoherent imaging [142], the effect of the finite size of the atom makes a clear difference in the relative intensities in the diffractogram: if the atoms can be considered as point objects—a reasonable approximation for HAADF–STEM with ultrathin samples—, the pure structure factors as shown in Fig. 6(b), damped by the finite resolution of the microscope, would show up on the Fourier transform of an image. However, for the bright-field STEM or HRTEM image, the diffracted intensities as in Fig. 6(c) are applicable instead, where the higher-order beams are already much weaker compared to the first-order ones. For a weakly scattering sample, this may make a difference for the visibility of the higher-order peaks.

Fig. 9 highlights the appearance of lattice resolution and atomic resolution in direct images. In order to create the lower-resolution example, we use a simulation to ensure that only the lowest order of diffracted beams (corresponding to a resolution of 2.13 Å) is transferred (Fig. 9(a)). The line profile is shown in Fig. 9(b): it may come as a surprise that there is a dip in-between the carbon atoms, spaced 1.42 Å apart, even though no information beyond 2 Å was allowed in this simulation. This is a peculiarity of the hexagonal structure; as long as no higher-order beams are transferred, this dip always appears with a height of ca. 7% of the total modulation. In other words, this small dip (Fig. 9(c)) must not be mistaken as evidence for a higher resolution. In contrast, Fig. 9(d) and (e) shows cases where higher-resolution information is definitely present in the images: the significantly stronger dip in-between the carbon atoms as visible here can only be present if a resolution of at least 1.23 Å is achieved.

8. Spectroscopy using electrons

Spectroscopic studies of nano-carbons by using electrons have been done with spatial resolutions ranging from angstroms to millimeters. If spatial resolution is not an issue, electron energy-loss spectroscopy (EELS) with high energy and momentum resolution can be carried out in special instruments (which are not electron microscopes) [143]. In this way, the plasmon dispersion of carbon nanotubes was measured, using a millimeter-sized sample [144]. Both localized and delocalized excitations were found, as expected for a one-dimensional solid. Using a TEM with a spectrometer, more local measurements become possible in a range of nanometers to microns [145–147]. For graphene, the difference between mono-layer and few-layer samples was shown already in some of the early STEM studies of this material [128,148], and the dispersion relation of plasmon excitation could be measured by angle-resolved EELS [149,150].

The angstrom-sized (or sub-angstrom-sized) probe of an aberration-corrected scanning transmission electron microscope provides not only a means to obtain high-resolution images, but also enables spectroscopic studies with single-atom or single-atomic-column resolution. Fig. 10 shows a high-resolution image of a graphene edge and electron-energy loss spectra that were recorded on the indicated positions (from Ref. [151]). Remarkably, it was possible to detect features in the fine structure of the spectra that can be associated with the undercoordinated carbon atoms at the edge [96,151].

Besides determining the bonding configuration of carbon from EELS, it is also possible to study the nature of single-atom impurities by spectroscopic means. For example, the interaction of deposited metals with graphene was studied and the nature of impurities was verified via EEL spectroscopy [152]. However, it appears that actually silicon is the most frequently found contamination across graphene samples made by different groups and different methods [132,133,140,153,154], even though its origin is not completely known. Two rather beam-stable configurations of this abundant contamination exist, replacing one or two carbon atoms [132,133], besides more complex configurations [153]. The element was identified by single-atom energy-dispersive X-ray spectroscopy (EDX) [154] as well as EELS [132,133,140,153,154], and the plasmon ex-
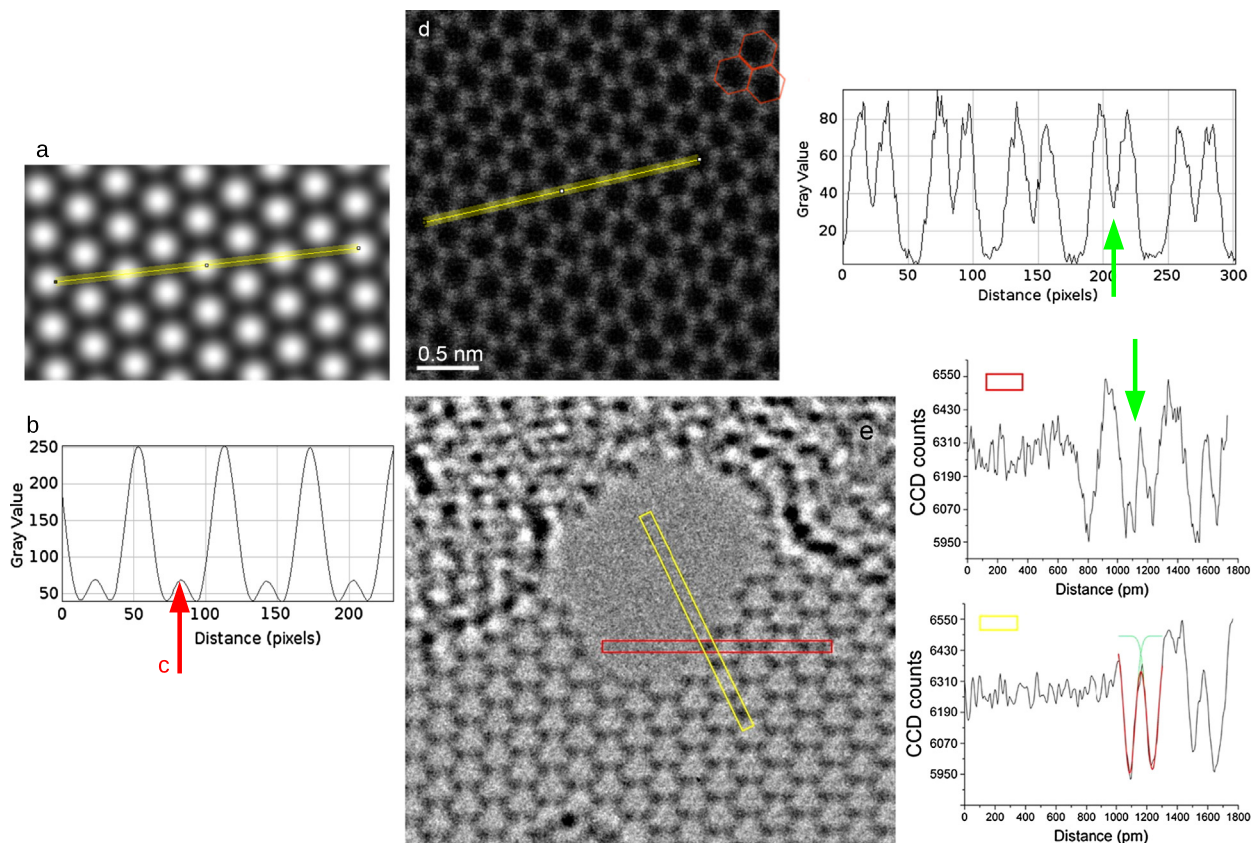
Fig. 9. (Color online.) Lattice resolution vs. atomic resolution. (a) Simulated image, where only the [1–100] reflection is transferred, and hence the resolution is 2.13 Å. (b) Line profile as indicated in (a). A small dip between the carbon atoms (ca. 7% of the total contrast, marked by an arrow (c)) is present already for this low resolution. (d) ADF–STEM image from Ref. [141], and a line profile. (e) Monochromated, AC–HRTEM image and line profiles from Ref. [138]. In both cases, the dip is significantly larger than 7% (green arrows), demonstrating a resolution well beyond the first reflection of the lattice. Fig. (d) adapted from Ref. [141], (e) reprinted with permission from Ref. [138], Copyright (2012) American Chemical Society.
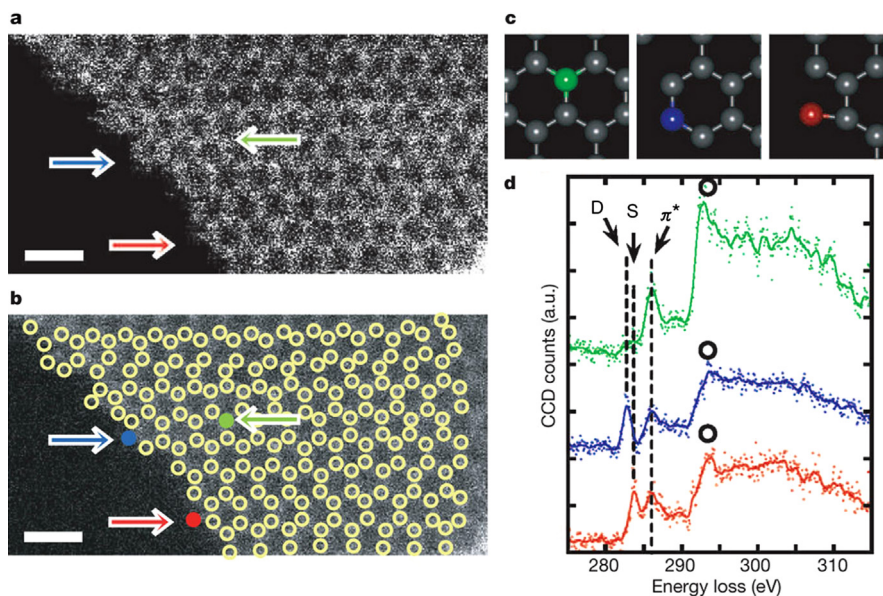

Fig. 10. (Color online.) A spectroscopic analysis of carbon atomic configurations at a graphene edge. The spectra obtained from under-coordinated atoms at the edge display distinctively different features as compared to the bulk atoms (Copyright (2010) Nature Publishing Group, reprinted with permission from Ref. [151]). Scale bar: 5 Å.
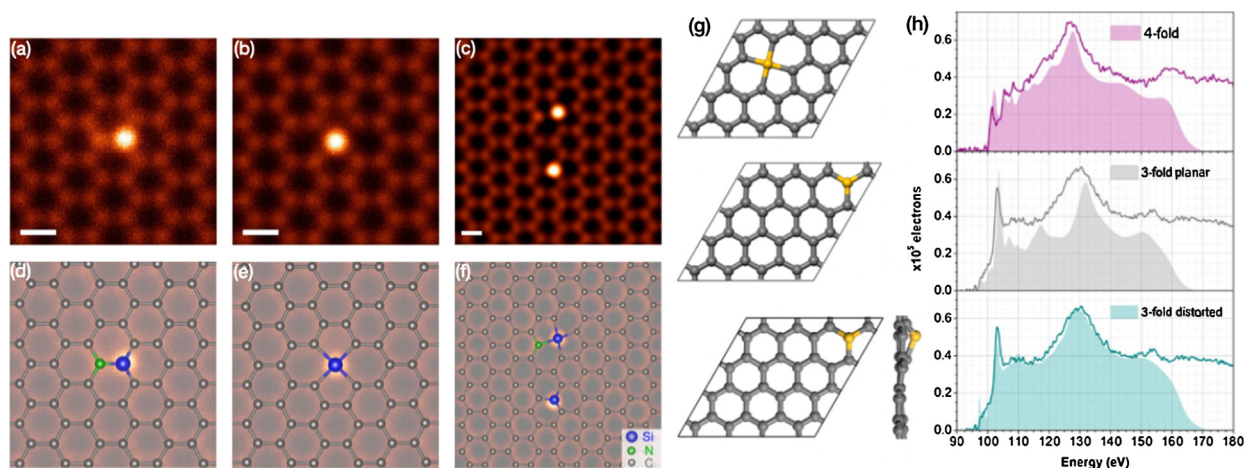
Fig. 11. (Color online.) STEM observation and EEL spectroscopy of individual silicon atoms in graphene. (a–f) STEM images and atomistic models as reported in Ref. [132]. (g–h) Simulated and experimental spectra as reported in Ref. [133]. It is important to note that the simulated spectra only match to the experiment if the out-of-plane position of the silicon atom is considered in the model. Scale bars in (a–c) are 0.2 nm. Images (a–f) are reprinted with permission from Ref. [132]. Copyright (2012) The American Physical Society, and (g–h) reprinted with permission from Ref. [133], Copyright (2012) The American Chemical Society.

citations in its surrounding were analyzed [140]. Remarkably, it is even possible to discern differences in bonding between the two configurations from EEL spectra of individual atoms, as found by two independent groups [132,133] and as shown in Fig. 11.

9. Carbon structures as sample support

In (HR)TEM and STEM, one of the crucial, but often less discussed issues is the matter of sample support. Usually any information obtained by the microscope is coming from interaction of the beam with the sample as well as with the support. Hence, one obviously wants to limit the contribution of the support as much as possible. Carbon has a long tradition as a support film for TEM samples due to the fact that its interaction with the electron beam is minimal since it is a light element. So it comes as no surprise that the vast majority of commercially available TEM support films incorporate some form of thin carbon layer—mostly supported by a metal grid. While in most cases an amorphous film of carbon is used, there are also reports of thin graphite support films in the early literature [155,156]. As already mentioned in Section 3 as the objects of interest to be studied by TEM decrease in size, the impact of the underlying support increases, leading to the need of thinner sample support films.

Besides conventional carbon films, low-dimensional carbon materials have received significant attention as potential TEM support films. The application of carbon nanotubes as nanoreactors became popular after the discovery of C-60 molecules trapped inside of carbon nanotubes [157], structures that became known as "fullerene peapods" [158–160]. Several authors have explored a filling of carbon nanotubes with other molecules (e.g., functionalized fullerenes [161–164], azafullerenes [165,166]) and subsequent reactions under heat or electron irradiation [167–172]. The confined space provides a means to form unique atomic structures inside the nanotubes [173–176], including graphene nanoribbons [177] and nanowires [178, 179]. Carbon nanotubes have further served as containers for imaging of biomolecules [180]. A review on this matter is given, e.g., in Ref. [163].

Graphene is a potentially ideal sample support since it is the thinnest material possible, it is highly conductive, very stable under lower-voltage irradiation, and has a well-known structure. Knowledge of the structure of graphene proves beneficial here, since if adsorbates on the graphene sheet are studied, the underlying lattice can be removed by a filter. The graphene lattice can also be facilitated as a built-in scale bar. On the other hand, the inert surface makes it difficult to attach objects of interest, and contamination turns out to be problematic. However, it should be pointed out that the contamination levels that are well visible on graphene would probably go unnoticed on other substrates. Indeed, several studies have shown the potential of graphene as TEM support by showing that contamination patches on graphene can be imaged with a remarkable signal-to-noise ratio [63,127,181–185]. Graphene films were shown to be beneficial for imaging of nanocrystals [186–188] and biomolecules [189–196]. Moreover, they turned out to be useful for in-situ experiments [197–199] where not only their transparency, but also mechanical and thermal stability is of high importance. Further, graphene was used for encapsulation of bacteria as a protection from irradiation [200], and for wet cell applications in SEM [201] and TEM [202].
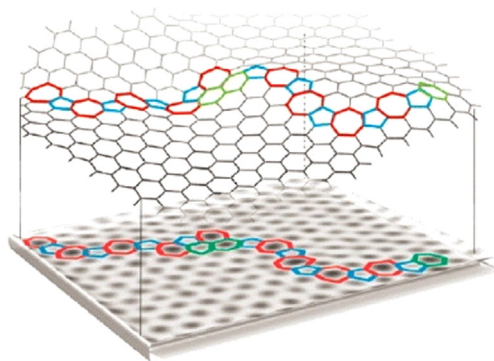
Fig. 12. (Color online.) Calculated out-of-plane deformations of an experimentally observed grain boundary [205]. So far, deformations in the third dimension were not experimentally measured for grain boundaries, dislocation dipoles or similar structures. Copyright (2011) The American Chemical Society, reprinted with permission from Ref. [205].

10. Graphene as the ideal test sample

Besides being the perfect sample support, there is another domain of carbon-based films in TEM applications, where graphene has the potential for deployment: application as a test sample for microscopic developments. A single-layer graphene sample is the *exact* same structure no matter how it was prepared or who made it. Moreover, the TEM and STEM images depend only weakly on sample tilt. Hence, it becomes possible to obtain precisely reproduced conditions on the side of the sample. Moreover, the single layer of carbon atoms is easy to model. Overall, this creates the possibility, that the contrast obtained from single-layer graphene may serve as a test criterion for instrumental performance and stability, e.g. by following and extending an analysis as in Fig. 9. By comparison with simulations, it may further serve to understand image contrast [104,117] or radiation damage [89]. Moreover, 2D samples such as graphene provide a comparatively easy way to measure spectroscopic signals of single atoms, including foreign species at point defects, as discussed above.

11. Summary and outlook

While the study of carbon materials by electron microscopy is nearly as old as electron microscopy itself, both fields have seen tremendous advances from developments in the past decade. In the area of carbon nanomaterials, the rise of graphene [203] has provided a new and fascinating object that is excellently suited for microscopic studies [204]. In the field of electron microscopy, the application and development of aberration-corrected instruments provided new avenues that were previously not conceivable. The developments towards low acceleration voltages made it possible to record images and spectra from individual light atoms. But since these developments are still ongoing, we may have only seen the tip of the iceberg so far. Although graphene is a 2D material, it is embedded in a 3D space and this third dimension has not been much explored so far: Fig. 12 shows calculated out-of-plane deformations [205,206] for a grain boundary that was observed experimentally in the projection of a high-resolution STEM image [76]. Similarly, out-of-plane deformations were calculated for observed dislocation dipole structures based on projection images [130,131]. With the projected atom density in graphene being sparse compared to the resolution of today's instruments, measurements of all three atomic coordinates appear to be within reach [207]. On the materials side, besides graphene there is also a rapidly growing interest in non-carbon 2D materials [208]. While microscopic studies of such structures have not been discussed here, they are similar to graphene in many aspects of high-resolution imaging, spectroscopic analysis, and sample preparation [209–213]. Chances are that we will see a growing fraction of studies related to non-carbon low-dimensional structures, which will benefit from the experience that was gained with studies of carbon nanotubes, graphene, and other nano-carbon forms.

References

[1] L. Radushkevich, V. Lukyanovich, O strukture ugleroda obrazujucegosja pri termiceskom razlozenii okisi ugleroda na zeleznom kontakte, Zh. Fiz. Khim. 26 (1952) 88.
[2] H. Hashimoto, R. Uyeda, Detection of dislocation by the moiré pattern in electron micrographs, Acta Crystallogr. 10 (Feb. 1957) 143.
[3] I.M. Dawson, E.A.C. Follett, An electron microscope study of synthetic graphite, Proc. R. Soc. Lond. Ser. A 253 (1274) (1959) 390–402.
[4] W. Bollmann, Electron microscope study of radiation damage in graphite, J. Appl. Phys. 32 (5) (1961) 869–876.
[5] F.E. Fujita, K. Izui, Observation of lattice defects in graphite by electron microscopy. Part I, J. Phys. Soc. Jpn. 16 (2) (1961) 214–227.
[6] J. Hedley, D. Ashworth, Imperfections in natural graphite, J. Nucl. Mater. 4 (May 1961) 70–78.
[7] H. Boehm, A. Clauss, G. Fischer, U. Hofmann, Surface properties of extremely thin graphite lamellae, in: Proceedings of the Fifth Conference on Carbon, vol. 1, 1962, pp. 73–80.
[8] S. Iijima, T. Ichihashi, Single-shell carbon nanotubes of 1-nm diameter, Nature 363 (June 1993) 603–605.
[9] S. Iijima, Helical microtubules of graphitic carbon, Nature 354 (Nov. 1991) 56–58.
[10] D.S. Bethune, C.H. Klang, M.S. de Vries, G. Gorman, R. Savoy, J. Vazquez, R. Beyers, Cobalt-catalysed growth of carbon nanotubes with single-atomic-layer walls, Nature 363 (June 1993) 605–607.

[11] K.S. Novoselov, A.K. Geim, S.V. Morozov, D. Jiang, Y. Zhang, S.V. Dubonos, I.V. Grigorieva, A.A. Firsov, Electric field effect in atomically thin carbon films, Science 306 (Oct. 2004) 666–669.

[12] H.W. Kroto, A.W. Allaf, S.P. Balm, C60: Buckminsterfullerene, Chem. Rev. 91 (6) (1991) 1213–1235.

[13] B. Eksioglu, A. Nadarajah, Structural analysis of conical carbon nanofibers, Carbon 44 (Feb. 2006) 360–373.

[14] J. Campos-Delgado, J.M. Romo-Herrera, X. Jia, D.A. Cullen, H. Muramatsu, Y.A. Kim, T. Hayashi, Z. Ren, D.J. Smith, Y. Okuno, T. Ohba, H. Kanoh, K. Kaneko, M. Endo, H. Terrones, M.S. Dresselhaus, M. Terrones, Bulk production of a new form of sp(2) carbon: crystalline graphene nanoribbons, Nano Lett. 8 (Sept. 2008) 2773–2778.

[15] X. Jia, M. Hofmann, V. Meunier, B.G. Sumpter, J. Campos-Delgado, J.M. Romo-Herrera, H. Son, Y.-P. Hsieh, A. Reina, J. Kong, M. Terrones, M.S. Dresselhaus, Controlled formation of sharp zigzag and armchair edges in graphitic nanoribbons, Science 323 (Mar. 2009) 1701–1705.

[16] D. Ugarte, Curling and closure of graphitic networks under electron-beam irradiation, Nature 359 (Oct. 1992) 707–709.

[17] Y. Saito, T. Yoshikawa, M. Inagaki, M. Tomita, T. Hayashi, Growth and structure of graphitic tubules and polyhedral particles in arc-discharge, Chem. Phys. Lett. 204 (Mar. 1993) 277–282.

[18] L.M. Viculis, J.J. Mack, R.B. Kaner, A chemical route to carbon nanoscrolls, Science 299 (Feb. 2003) 1361.

[19] C. Jin, H. Lan, L. Peng, K. Suenaga, S. Iijima, Deriving carbon atomic chains from graphene, Phys. Rev. Lett. 102 (May 2009) 205501.

[20] A. Chuvilin, J.C. Meyer, G. Algara-Siller, U. Kaiser, From graphene constrictions to single carbon chains, New J. Phys. 11 (Aug. 2009) 083019.

[21] O. Cretu, A.R. Botello-Mendez, I. Janowska, C. Pham-Huu, J.-C. Charlier, F. Banhart, Electrical transport measured in atomic carbon chains, Nano Lett. (July 2013).

[22] S. Subramoney, Novel nanocarbons—structure, properties, and potential applications, Adv. Mater. 10 (15) (1998) 1157–1171.

[23] K. Nagayama, R. Danev, Phase-plate electron microscopy: a novel imaging tool to reveal close-to-life nano-structures, Biophys. Rev. 1 (Mar. 2009) 37–42.

[24] T. Hanai, M. Hibino, S. Maruse, Improvement of an electron probe profile using the foil lens, Microscopy (Tokyo) 31 (Jan. 1982) 360–367.

[25] S. Sugiyama, M. Hibino, S. Maruse, Transmission rate of electrons for carbon films used as the foil of the foil lens, Microscopy (Tokyo) 33 (Jan. 1984) 323–328.

[26] Z. Wang, P. Poncharal, W. de Heer, Measuring physical and mechanical properties of individual carbon nanotubes by in situ TEM, J. Phys. Chem. Solids 61 (July 2000) 1025–1030.

[27] Z.L. Wang, R.P. Gao, W.A. de Heer, P. Poncharal, In situ imaging of field emission from individual carbon nanotubes and their structural damage, Appl. Phys. Lett. 80 (Feb. 2002) 856.

[28] J. Cumings, A. Zettl, M. McCartney, J. Spence, Electron holography of field-emitting carbon nanotubes, Phys. Rev. Lett. 88 (Jan. 2002) 056804.

[29] N. de Jonge, Y. Lamy, K. Schoots, T.H. Oosterkamp, High brightness electron beam from a multi-walled carbon nanotube, Nature 420 (Nov. 2002) 393–395.

[30] J. Cumings, A. Zettl, M.R. McCartney, Carbon nanotube electrostatic biprism: principle of operation and proof of concept, Microsc. Microanal. 10 (Aug. 2004) 420–424.

[31] A. Krueger, M. Ozawa, F. Banhart, Carbon nanotubes as elements to focus electron beams by Fresnel diffraction, Appl. Phys. Lett. 83 (Dec. 2003) 5056.

[32] T. Oku, I. Narita, A. Nishiwaki, Formation, atomic structural optimization and electronic structures of tetrahedral carbon onion, Diam. Relat. Mater. 13 (Apr. 2004) 1337–1341.

[33] S. Iijima, Carbon nanotubes: past, present, and future, Physica B, Condens. Matter 323 (Oct. 2002) 1–5.

[34] J. Kotakoski, A.V. Krasheninnikov, U. Kaiser, J.C. Meyer, From point defects in graphene to two-dimensional amorphous carbon, Phys. Rev. Lett. 106 (Mar. 2011) 105505.

[35] P.J.F. Harris, Z. Liu, K. Suenaga, Imaging the atomic structure of activated carbon, J. Phys. Condens. Matter 20 (Sept. 2008) 362201.

[36] V.H. Crespi, L.X. Benedict, M.L. Cohen, S.G. Louie, Prediction of a pure-carbon planar covalent metal, Phys. Rev. B 53 (May 1996) R13303–R13305.

[37] X. Sheng, H. Cui, F. Ye, Q. Yan, Q. Zheng, G. Su, Octagraphene as a versatile carbon atomic sheet for novel nanotubes, unconventional fullerenes, and hydrogen storage, J. Appl. Phys. 112 (Oct. 2012) 074315 (7 pp.).

[38] M.T. Lusk, L.D. Carr, Nanoengineering defect structures on graphene, Phys. Rev. Lett. 100 (Apr. 2008) 175503.

[39] H. Terrones, M. Terrones, E. Hernández, N. Grobert, J. Charlier, P.M. Ajayan, New metallic allotropes of planar and tubular carbon, Phys. Rev. Lett. 84 (Feb. 2000) 1716–1719.

[40] J. Hedley, D. Ashworth, Imperfections in natural graphite, J. Nucl. Mater. 4 (May 1961) 70–78.

[41] M. Isaacson, M. Ohtsuki, M. Utlaut, Can we determine the structure of thin amorphous film using scanning transmission electron microscopy, in: Proceedings of the 37th Annual EMSA Meeting, 1979, pp. 498–501.

[42] M.S. Isaacson, Seeing single atoms, Ultramicroscopy 123 (Dec. 2012) 3–12.

[43] A.V. Crewe, High-resolution scanning transmission electron microscopy, Science 221 (July 1983) 325–330.

[44] A. Oberlin, M. Endo, T. Koyama, Filamentous growth of carbon through benzene decomposition, J. Cryst. Growth 32 (Mar. 1976) 335–349.

[45] J. Prasek, J. Drbohlavova, J. Chomoucka, J. Hubalek, O. Jasek, V. Adam, R. Kizek, Methods for carbon nanotubes synthesis—review, J. Mater. Chem. 21 (Oct. 2011) 15872–15884.

[46] X. Wang, W. Hu, Y. Liu, C. Long, Y. Xu, S. Zhou, D. Zhu, L. Dai, Bamboo-like carbon nanotubes produced by pyrolysis of iron(II) phthalocyanine, Carbon 39 (Aug. 2001) 1533–1536.

[47] A.Y. Kasumov, Supercurrents through single-walled carbon nanotubes, Science 284 (May 1999) 1508–1511.

[48] M. Kociak, K. Suenaga, K. Hirahara, Y. Saito, T. Nakahira, S. Iijima, Linking chiral indices and transport properties of double-walled carbon nanotubes, Phys. Rev. Lett. 89 (Sept. 2002) 155501.

[49] A.M. Fennimore, T.D. Yuzvinsky, W.-Q. Han, M.S. Fuhrer, J. Cumings, A. Zettl, Rotational actuators based on carbon nanotubes, Nature 424 (July 2003) 408–410.

[50] J. Meyer, D. Obergfell, S. Roth, S. Yang, Transmission electron microscopy and transistor characteristics of the same carbon nanotube, Appl. Phys. Lett. 85 (14) (2004) 2911.

[51] J.C. Meyer, M. Paillet, S. Roth, Single-molecule torsional pendulum, Science 309 (Sept. 2005) 1539–1541.

[52] J. Meyer, M. Paillet, T. Michel, A. Moréac, A. Neumann, G. Duesberg, S. Roth, J. Sauvajol, Raman modes of index-identified freestanding single-walled carbon nanotubes, Phys. Rev. Lett. 95 (21) (2005) 217401.

[53] J.C. Meyer, M. Paillet, G.S. Duesberg, S. Roth, Electron diffraction analysis of individual single-walled carbon nanotubes, Ultramicroscopy 106 (Feb. 2006) 176–190.

[54] A. Jungen, S. Hofmann, J.C. Meyer, C. Stampfer, S. Roth, J. Robertson, C. Hierold, Synthesis of individual single-walled carbon nanotube bridges controlled by support micromachining, J. Micromech. Microeng. 17 (2007) 603–608.

[55] S. Helveg, C. López-Cartes, J. Sehested, P.L. Hansen, B.S. Clausen, J.R. Rostrup-Nielsen, F. Abild-Pedersen, J. Nørskov, Atomic-scale imaging of carbon nanofibre growth, Nature 427 (Jan. 2004) 426–429.

[56] R. Sharma, Z. Iqbal, In situ observations of carbon nanotube formation using environmental transmission electron microscopy, Appl. Phys. Lett. 84 (Feb. 2004) 990.

[57] S. Hofmann, R. Sharma, C. Ducati, G. Du, C. Mattevi, C. Cepek, M. Cantoro, S. Pisana, A. Parvez, F. Cervantes-Sodi, A.C. Ferrari, R. Dunin-Borkowski, S. Lizzit, L. Petaccia, A. Goldoni, J. Robertson, In situ observations of catalyst dynamics during surface-bound carbon nanotube nucleation, Nano Lett. 7 (Mar. 2007) 602–608.

[58] J. Park, G. Choi, Y. Cho, S. Hong, D. Kim, S. Choi, J. Lee, K. Cho, Characterization of Fe-catalyzed carbon nanotubes grown by thermal chemical vapor deposition, J. Cryst. Growth 244 (Oct. 2002) 211–217.

[59] X. Ke, S. Bals, A. Romo Negreira, T. Hantschel, H. Bender, G. Van Tendeloo, TEM sample preparation by FIB for carbon nanotube interconnects, Ultramicroscopy 109 (Oct. 2009) 1353–1359.

[60] P. Blake, E.W. Hill, A.H. Castro Neto, K.S. Novoselov, D. Jiang, R. Yang, T.J. Booth, A.K. Geim, Making graphene visible, Appl. Phys. Lett. 91 (Aug. 2007) 063124.

[61] J. Meyer, A. Geim, M. Katsnelson, K. Novoselov, D. Obergfell, S. Roth, C. Girit, A. Zettl, On the roughness of single- and bi-layer graphene membranes, Solid State Commun. 143 (July 2007) 101–109.

[62] J.C. Meyer, A.K. Geim, M.I. Katsnelson, K.S. Novoselov, T.J. Booth, S. Roth, The structure of suspended graphene sheets, Nature 446 (Mar. 2007) 60–63.

[63] T.J. Booth, P. Blake, R.R. Nair, D. Jiang, E.W. Hill, U. Bangert, A. Bleloch, M. Gass, K.S. Novoselov, M.I. Katsnelson, A.K. Geim, Macroscopic graphene membranes and their extraordinary stiffness, Nano Lett. 8 (Aug. 2008) 2442–2446.

[64] R.R. Nair, P. Blake, A.N. Grigorenko, K.S. Novoselov, T.J. Booth, T. Stauber, N.M.R. Peres, A.K. Geim, Fine structure constant defines visual transparency of graphene, Science 320 (June 2008) 1308.

[65] J.C. Meyer, C.O. Girit, M.F. Crommie, A. Zettl, Hydrocarbon lithography on graphene membranes, Appl. Phys. Lett. 92 (Mar. 2008) 123110–123113.

[66] C. Gómez-Navarro, J.C. Meyer, R.S. Sundaram, A. Chuvilin, S. Kurasch, M. Burghard, K. Kern, U. Kaiser, Atomic structure of reduced graphene oxide, Nano Lett. 10 (Apr. 2010) 1144–1148.

[67] K. Erickson, R. Erni, Z. Lee, N. Alem, W. Gannett, A. Zettl, Determination of the local chemical structure of graphene oxide and reduced graphene oxide, Adv. Mater. 22 (Aug. 2010) 4467–4472.

[68] D. Pacilé, J. Meyer, A. Fraile Rodríguez, M. Papagno, C. Gómez-Navarro, R. Sundaram, M. Burghard, K. Kern, C. Carbone, U. Kaiser, Electronic properties and atomic structure of graphene oxide membranes, Carbon 49 (Mar. 2011) 966–972.

[69] Q. Yu, J. Lian, S. Siriponglert, H. Li, Y.P. Chen, S. Pei, Graphene segregated on Ni surfaces and transferred to insulators, Appl. Phys. Lett. 93 (Sept. 2008) 113101 (3 pp.).

[70] A. Reina, X. Jia, J. Ho, D. Nezich, H. Son, V. Bulovic, M.S. Dresselhaus, J. Kong, Large area, few-layer graphene films on arbitrary substrates by chemical vapor deposition, Nano Lett. 9 (Jan. 2009) 30–35.

[71] X. Li, W. Cai, J. An, S. Kim, J. Nah, D. Yang, R. Piner, A. Velamakanni, I. Jung, E. Tutuc, S.K. Banerjee, L. Colombo, R.S. Ruoff, Large-area synthesis of high-quality and uniform graphene films on copper foils, Science 324 (June 2009) 1312–1314.

[72] B. Alemán, W. Regan, S. Aloni, V. Altoe, N. Alem, C. Girit, B. Geng, L. Maserati, M. Crommie, F. Wang, A. Zettl, Transfer-free batch fabrication of large-area suspended graphene membranes, ACS Nano 4 (Aug. 2010) 4762–4768.

[73] H.J. Park, J.C. Meyer, S. Roth, V. Skakalova, Growth and properties of few-layer graphene prepared by chemical vapor deposition, Carbon 48 (4) (2010) 1088–1094.

[74] Y.-C. Lin, C.-C. Lu, C.-H. Yeh, C. Jin, K. Suenaga, P.-W. Chiu, Graphene annealing: How clean can it be? Nano Lett. 12 (1) (2012) 414–419.

[75] Y. Lin, C. Jin, J. Lee, S. Jen, K. Suenaga, P. Chiu, Clean transfer of graphene for isolation and suspension, ACS Nano 5 (Mar. 2011) 2362–2368.

[76] P.Y. Huang, C.S. Ruiz-Vargas, A.M. van der Zande, W.S. Whitney, M.P. Levendorf, J.W. Kevek, S. Garg, J.S. Alden, C.J. Hustedt, Y. Zhu, J. Park, P.L. McEuen, D.A. Muller, Grains and grain boundaries in single-layer graphene atomic patchwork quilts, Nature 469 (Jan. 2011) 389–392.

[77] S.J. Haigh, A. Gholinia, R. Jalil, S. Romani, L. Britnell, D.C. Elias, K.S. Novoselov, L.A. Ponomarenko, A.K. Geim, R. Gorbachev, Cross-sectional imaging of individual layers and buried interfaces of graphene-based heterostructures and superlattices, Nat. Mater. 11 (July 2012) 9–12.

[78] A. Ansaldo, M. Haluska, J. Cech, J. Meyer, D. Ricci, F. Gatti, E. Di Zitti, S. Cincotti, S. Roth, A study of the effect of different catalysts for the efficient CVD growth of carbon nanotubes on silicon substrates, Physica E, Low-Dimens. Syst. Nanostruct. 37 (1–2) (2007) 6–10.

[79] M. Yu, O. Lourie, M.J. Dyer, K. Moloni, T.F. Kelly, R.S. Ruoff, Strength and breaking mechanism of multiwalled carbon nanotubes under tensile load, Science 287 (Jan. 2000) 637–640.

[80] R.Y. Zhang, Y. Wei, L.A. Nagahara, I. Amlani, R.K. Tsui, The contrast mechanism in low voltage scanning electron microscopy of single-walled carbon nanotubes, Nanotechnology 17 (Jan. 2006) 272–276.

[81] M. Lucas, E. Mitchell, The threshold curve for the displacement of atoms in graphite: Experiments on the resistivity changes produced in single crystals by fast electron irradiation at 15 K, Carbon 1 (Apr. 1964) 345–352.

[82] V.H. Crespi, N.G. Chopra, M.L. Cohen, A. Zettl, S. Louie, Anisotropic electron-beam damage and the collapse of carbon nanotubes, Phys. Rev. B Condens. Matter 54 (Aug. 1996) 5927–5931.

[83] F. Banhart, Irradiation effects in carbon nanostructures, Rep. Prog. Phys. 62 (1999) 1181.

[84] B.W. Smith, D.E. Luzzi, Electron irradiation effects in single wall carbon nanotubes, J. Appl. Phys. 90 (Oct. 2001) 3509–3515.

[85] A. Krasheninnikov, F. Banhart, J. Li, A. Foster, R. Nieminen, Stability of carbon nanotubes under electron irradiation: Role of tube diameter and chirality, Phys. Rev. B 72 (Sept. 2005).

[86] A. Zobelli, A. Gloter, C. Ewels, G. Seifert, C. Colliex, Electron knock-on cross section of carbon and boron nitride nanotubes, Phys. Rev. B 75 (June 2007) 1–9.

[87] K. Mølhave, S.B. Gudnason, A.T. Pedersen, C.H. Clausen, A. Horsewell, P. Bøggild, Electron irradiation-induced destruction of carbon nanotubes in electron microscopes, Ultramicroscopy 108 (Dec. 2007) 52–57.

[88] J.H. Warner, F. Schäffel, G. Zhong, M.H. Rümmeli, B. Büchner, J. Robertson, G.A.D. Briggs, Investigating the diameter-dependent stability of single-walled carbon nanotubes, ACS Nano 3 (June 2009) 1557–1563.

[89] J.C. Meyer, F. Eder, S. Kurasch, V. Skakalova, J. Kotakoski, H.J. Park, S. Roth, A. Chuvilin, S. Eyhusen, G. Benner, A.V. Krasheninnikov, U. Kaiser, Accurate measurement of electron beam induced displacement cross sections for single-layer graphene, Phys. Rev. Lett. 108 (May 2012) 196102.

[90] A. Santana, A. Zobelli, J. Kotakoski, A. Chuvilin, E. Bichoutskaia, Inclusion of radiation damage dynamics in high-resolution transmission electron microscopy image simulations: The example of graphene, Phys. Rev. B 87 (Mar. 2013) 094110.

[91] T.D. Yuzvinsky, A.M. Fennimore, W. Mickelson, C. Esquivias, A. Zettl, Precision cutting of nanotubes with a low-energy electron beam, Appl. Phys. Lett. 86 (5) (2005) 053109.

[92] H. Sawada, T. Sasaki, F. Hosokawa, S. Yuasa, M. Terao, M. Kawazoe, T. Nakamichi, T. Kaneyama, Y. Kondo, K. Kimoto, K. Suenaga, Higher-order aberration corrector for an image-forming system in a transmission electron microscope, Ultramicroscopy 110 (July 2010) 958–961.

[93] U. Kaiser, J. Biskupek, J. Meyer, J. Leschner, L. Lechner, H. Rose, M. Stöger-Pollach, A. Khlobystov, P. Hartel, H. Müller, M. Haider, S. Eyhusen, G. Benner, Transmission electron microscopy at 20 kV for imaging and spectroscopy, Ultramicroscopy 111 (July 2011) 1239–1246.

[94] O.L. Krivanek, N. Dellby, M.F. Murfitt, M.F. Chisholm, T.J. Pennycook, K. Suenaga, V. Nicolosi, Gentle STEM: ADF imaging and EELS at low primary energies, Ultramicroscopy 110 (July 2010) 935–945.

[95] J. Kotakoski, J.C. Meyer, S. Kurasch, D. Santos-Cottin, U. Kaiser, A.V. Krasheninnikov, Stone–Wales-type transformations in carbon nanostructures driven by electron irradiation, Phys. Rev. B 83 (June 2011) 245420.

[96] C. Colliex, A. Gloter, K. March, C. Mory, O. Stéphan, K. Suenaga, M. Tencé, Capturing the signature of single atoms with the tiny probe of a STEM, Ultramicroscopy 123 (Dec. 2012) 80–89.

[97] A.V. Krasheninnikov, F. Banhart, Engineering of nanostructured carbon materials with electron or ion beams, Nat. Mater. 6 (10) (2007) 723–733.

[98] A. Zobelli, A. Gloter, C. Ewels, C. Colliex, Shaping single walled nanotubes with an electron beam, Phys. Rev. B 77 (Jan. 2008) 1–8.

[99] J.A. Rodriguez-Manzo, F. Banhart, Creation of individual vacancies in carbon nanotubes by using an electron beam of 1 Å diameter, Nano Lett. 9 (June 2009) 2285–2289.

[100] M.D. Fischbein, M. Drndic, Electron beam nanosculpting of suspended graphene sheets, Appl. Phys. Lett. 93 (Sept. 2008) 113107.

[101] J. Li, F. Banhart, The engineering of hot carbon nanotubes with a focused electron beam, Nano Lett. 4 (June 2004) 1143–1146.

[102] B. Song, G.F. Schneider, Q. Xu, G. Pandraud, C. Dekker, H. Zandbergen, Atomic-scale electron-beam sculpting of near-defect-free graphene nanostructures, Nano Lett. 11 (June 2011) 2247–2250.

[103] F. Banhart, J. Li, M. Terrones, Cutting single-walled carbon nanotubes with an electron beam: evidence for atom migration inside nanotubes, Small 1 (Oct. 2005) 953–956.

[104] Z. Lee, J. Meyer, H. Rose, U. Kaiser, Optimum HRTEM image contrast at 20 kV and 80 kV-exemplified by graphene, Ultramicroscopy 112 (Jan. 2012) 39–46.

[105] J.R. Jinschek, E. Yucelen, H.A. Calderon, B. Freitag, Quantitative atomic 3-D imaging of single/double sheet graphene structure, Carbon 49 (Feb. 2011) 556–562.

[106] A.A. Lucas, V. Bruyninckx, P. Lambin, D. Bernaerts, S. Amelinckx, J.V. Landuyt, G.V. Tendeloo, Electron diffraction by carbon nanotubes, Scanning Microsc. 12 (3) (1998) 415–436.

[107] A.A. Lucas, P. Lambin, Diffraction by DNA, carbon nanotubes and other helical nanostructures, Rep. Prog. Phys. 68 (May 2005) 1181–1249.

[108] M. Gao, J.M. Zuo, R.D. Twesten, I. Petrov, L.A. Nagahara, R. Zhang, Structure determination of individual single-wall carbon nanotubes by nanoarea electron diffraction, Appl. Phys. Lett. 82 (16) (2003) 2703.

[109] X. Zhang, X. Zhang, S. Amelinckx, G. Van Tendeloo, J. Van Landuyt, The reciprocal space of carbon tubes: a detailed interpretation of the electron diffraction effects, Ultramicroscopy 54 (June 1994) 237–249.

[110] Z. Liu, L.-C. Qin, A direct method to determine the chiral indices of carbon nanotubes, Chem. Phys. Lett. 408 (June 2005) 75–79.

[111] P. Lambin, A. Lucas, Quantitative theory of diffraction by carbon nanotubes, Phys. Rev. B 56 (Aug. 1997) 3571–3574.

[112] J.M. Zuo, I. Vartanyants, M. Gao, R. Zhang, L.A. Nagahara, Atomic resolution imaging of a carbon nanotube from diffraction intensities, Science 300 (May 2003) 1419–1421.

[113] C. Qin, L.-M. Peng, Measurement accuracy of the diameter of a carbon nanotube from TEM images, Phys. Rev. B 65 (Apr. 2002) 1–7.

[114] L.-C. Qin, Electron diffraction from carbon nanotubes, Rep. Prog. Phys. 69 (Oct. 2006) 2761–2821.

[115] Z. Liu, L.-C. Qin, Electron diffraction from elliptical nanotubes, Chem. Phys. Lett. 406 (Apr. 2005) 106–110.

[116] Z. Liu, L.-C. Qin, Measurement of handedness in multiwalled carbon nanotubes by electron diffraction, Chem. Phys. Lett. 411 (Aug. 2005) 291–296.

[117] J.C. Meyer, S. Kurasch, H.J. Park, V. Skakalova, D. Künzel, A. Groß, A. Chuvilin, G. Algara-Siller, S. Roth, T. Iwasaki, U. Starke, J.H. Smet, U. Kaiser, Experimental analysis of charge redistribution due to chemical bonding by high-resolution transmission electron microscopy, Nat. Mater. 10 (Mar. 2011) 209–215.

[118] K. Kim, Z. Lee, W. Regan, C. Kisielowski, M.F. Crommie, A. Zettl, Grain boundary mapping in polycrystalline graphene, ACS Nano 5 (Mar. 2011) 2142–2146.

[119] L. Brown, R. Hovden, P. Huang, M. Wojcik, D.A. Muller, J. Park, Twinning and twisting of tri- and bilayer graphene, Nano Lett. 12 (Mar. 2012) 1609–1615.

[120] D. Kirilenko, A. Dideykin, G. Van Tendeloo, Measuring the corrugation amplitude of suspended and supported graphene, Phys. Rev. B 84 (Dec. 2011) 235417.

[121] A.W. Tsen, L. Brown, M.P. Levendorf, F. Ghahari, P.Y. Huang, R.W. Havener, C.S. Ruiz-Vargas, D.A. Muller, P. Kim, J. Park, Tailoring electrical transport across grain boundaries in polycrystalline graphene, Science (New York, NY) 336 (June 2012) 1143–1146.

[122] R.R. Meyer, S. Friedrichs, A.I. Kirkland, J. Sloan, J.L. Hutchison, M.L.H. Green, A composite method for the determination of the chirality of single walled carbon nanotubes, J. Microsc. 212 (Nov. 2003) 152–157.

[123] A. Hashimoto, K. Suenaga, A. Gloter, K. Urita, S. Iijima, Direct evidence for atomic defects in graphene layers, Nature 430 (Aug. 2004) 870–873.

[124] M. Haider, S. Uhlemann, E. Schwan, H. Rose, B. Kabius, K. Urban, Electron microscopy image enhanced, Nature 392 (Apr. 1998) 768–769.

[125] P.E. Batson, N. Dellby, O.L. Krivanek, Sub-ångstrom resolution using aberration corrected electron optics, Nature 418 (Aug. 2002) 617–620.

[126] K. Suenaga, H. Wakabayashi, M. Koshino, Y. Sato, K. Urita, S. Iijima, Imaging active topological defects in carbon nanotubes, Nat. Nanotechnol. 2 (June 2007) 358–360.

[127] J.C. Meyer, C.O. Girit, M.F. Crommie, A. Zettl, Imaging and dynamics of light atoms and molecules on graphene, Nature 454 (July 2008) 319–322.

[128] M.H. Gass, U. Bangert, A.L. Bleloch, P. Wang, R.R. Nair, A.K. Geim, Free-standing graphene at atomic resolution, Nat. Nanotechnol. 3 (Nov. 2008) 676–681.

[129] J.C. Meyer, C. Kisielowski, R. Erni, M.D. Rossell, M.F. Crommie, A. Zettl, Direct imaging of lattice atoms and topological defects in graphene membranes, Nano Lett. 8 (Nov. 2008) 3582–3586.

[130] J.H. Warner, E.R. Margine, M. Mukai, A.W. Robertson, F. Giustino, A.I. Kirkland, Dislocation-driven deformations in graphene, Science 337 (July 2012) 209–212.

[131] O. Lehtinen, S. Kurasch, A.V. Krasheninnikov, U. Kaiser, Atomic scale study of the life cycle of a dislocation in graphene from birth to annihilation, Nat. Commun. 4 (June 2013) 2098.

[132] W. Zhou, M.D. Kapetanakis, M.P. Prange, S.T. Pantelides, S.J. Pennycook, J.-C. Idrobo, Direct determination of the chemical bonding of individual impurities in graphene, Phys. Rev. Lett. 109 (Nov. 2012) 206803.

[133] Q.M. Ramasse, C.R. Seabourne, D. Kepaptsoglou, R. Zan, U. Bangert, A.J. Scott, Probing the bonding and electronic structure of single atom dopants in graphene with electron energy loss spectroscopy, Nano Lett. 13 (10) (2013) 4989–4995.

[134] H. Amara, S. Latil, V. Meunier, P. Lambin, J. Charlier, Scanning tunneling microscopy fingerprints of point defects in graphene: A theoretical prediction, Phys. Rev. B 76 (Sept. 2007) 115423.

[135] A. Stone, D. Wales, Theoretical studies of icosahedral c60 and some related species, Chem. Phys. Lett. 128 (Aug. 1986) 501–503.

[136] G. Lee, C.Z. Wang, E. Yoon, N. Hwang, D. Kim, K.M. Ho, Diffusion, coalescence, and reconstruction of vacancy defects in graphene layers, Phys. Rev. Lett. 95 (Nov. 2005) 205501.

[137] B.W. Jeong, J. Ihm, G. Lee, Stability of dislocation defect with two pentagon–heptagon pairs in graphene, Phys. Rev. B 78 (Oct. 2008) 1654.

[138] J.H. Warner, M. Mukai, A.I. Kirkland, Atomic structure of ABC rhombohedral stacked trilayer graphene, ACS Nano 6 (June 2012) 5680–5686.

[139] O.L. Krivanek, M.F. Chisholm, V. Nicolosi, T.J. Pennycook, G.J. Corbin, N. Dellby, M.F. Murfitt, C.S. Own, Z.S. Szilagyi, M.P. Oxley, S.T. Pantelides, S.J. Pennycook, Atom-by-atom structural and chemical analysis by annular dark-field electron microscopy, Nature 464 (Mar. 2010) 571–574.

[140] W. Zhou, J. Lee, J. Nanda, S.T. Pantelides, S.J. Pennycook, J. Idrobo, Atomically localized plasmon enhancement in monolayer graphene, Nat. Nanotechnol. 7 (Mar. 2012) 161–165.

[141] R.J. Recep Zan, Quentin M. Ramasse, U. Bangert, Advances in Graphene Science, InTech, July 2013.

[142] S. Van Aert, D. Van Dyck, A.J. den Dekker, Resolution of coherent and incoherent imaging systems reconsidered – Classical criteria and a statistical alternative, Opt. Express 14 (May 2006) 3830.

[143] J. Fink, Advances in Electronics and Electron Physics, vol. 75, Elsevier, 1989.
[144] T. Pichler, M. Knupfer, M. Golden, J. Fink, A. Rinzler, R. Smalley, Localized and delocalized electronic states in single-wall carbon nanotubes, Phys. Rev. Lett. 80 (May 1998) 4729–4732.
[145] R. Kuzuo, M. Terauchi, M. Tanaka, Electron energy-loss spectra of carbon nanotubes, Jpn. J. Appl. Phys. 31 (Oct. 1992) L1484–L1487.
[146] S. Tomita, M. Fujii, S. Hayashi, K. Yamamoto, Electron energy-loss spectroscopy of carbon onions, Chem. Phys. Lett. 305 (May 1999) 225–229.
[147] O. Stéphan, P. Ajayan, C. Colliex, F. Cyrot-Lackmann, E. Sandré, Curvature-induced bonding changes in carbon nanotubes investigated by electron energy-loss spectrometry, Phys. Rev. B 53 (May 1996) 13824–13829.
[148] T. Eberlein, U. Bangert, R. Nair, R. Jones, M. Gass, A. Bleloch, K. Novoselov, A. Geim, P. Briddon, Plasmon spectroscopy of free-standing graphene films, Phys. Rev. B 77 (June 2008) 1–4.
[149] M.K. Kinyanjui, C. Kramberger, T. Pichler, J.C. Meyer, P. Wachsmuth, G. Benner, U. Kaiser, Direct probe of linearly dispersing 2D interband plasmons in a free-standing graphene monolayer, Europhys. Lett. 97 (Mar. 2012) 57005.
[150] P. Wachsmuth, R. Hambach, M.K. Kinyanjui, M. Guzzo, G. Benner, U. Kaiser, High-energy collective electronic excitations in free-standing single-layer graphene, Phys. Rev. B 88 (Aug. 2013) 075433.
[151] K. Suenaga, M. Koshino, Atom-by-atom spectroscopy at graphene edge, Nature 468 (Dec. 2010) 1088–1090.
[152] Q.M. Ramasse, R. Zan, U. Bangert, D.W. Boukhvalov, Y.-W. Son, K.S. Novoselov, Direct experimental evidence of metal-mediated etching of suspended graphene, ACS Nano 6 (May 2012) 4063–4071.
[153] J. Lee, W. Zhou, S.J. Pennycook, J.-C. Idrobo, S.T. Pantelides, Direct visualization of reversible dynamics in a Si cluster embedded in a graphene pore, Nat. Commun. 4 (Jan. 2013) 1650.
[154] T.C. Lovejoy, Q.M. Ramasse, M. Falke, A. Kaeppel, R. Terborg, R. Zan, N. Dellby, O.L. Krivanek, Single atom identification by energy dispersive X-ray spectroscopy, Appl. Phys. Lett. 100 (Apr. 2012) 154101 (4 pp.).
[155] W.H. Dobelle, M. Beer, Chemically cleaved graphite support films for electron microscopy, J. Cell Biol. 39 (3) (1968) 733–735.
[156] S. Iijima, Thin graphite support films for high resolution electron microscopy, Micron (1969) 8 (1–2) (1977) 41–46.
[157] B.W. Smith, M. Monthioux, D.E. Luzzi, Encapsulated C60 in carbon nanotubes, Nature 396 (Nov. 1998) 323–324.
[158] C.S. Allen, Y. Ito, A.W. Robertson, H. Shinohara, J.H. Warner, Two-dimensional coalescence dynamics of encapsulated metallofullerenes in carbon nanotubes, ACS Nano 5 (Dec. 2011) 10084–10089.
[159] K. Hirahara, K. Suenaga, S. Bandow, H. Kato, T. Okazaki, H. Shinohara, S. Iijima, One-dimensional metallofullerene crystal generated inside single-walled carbon nanotubes, Phys. Rev. Lett. 85 (Dec. 2000) 5384–5387.
[160] K. Hirahara, S. Bandow, K. Suenaga, H. Kato, T. Okazaki, H. Shinohara, S. Iijima, Electron diffraction study of one-dimensional crystals of fullerenes, Phys. Rev. B 64 (Aug. 2001) 115420.
[161] A.N. Khlobystov, K. Porfyrakis, M. Kanai, D.A. Britz, A. Ardavan, H. Shinohara, T.J.S. Dennis, G.A.D. Briggs, Molecular motion of endohedral fullerenes in single-walled carbon nanotubes, Angew. Chem., Int. Ed. Engl. 43 (Mar. 2004) 1386–1389.
[162] A.N. Khlobystov, D.A. Britz, G.A.D. Briggs, Molecules in carbon nanotubes, Acc. Chem. Res. 38 (Dec. 2005) 901–909.
[163] A.N. Khlobystov, Carbon nanotubes: From nano test tube to nano-reactor, ACS Nano 5 (Dec. 2011) 9306–9312.
[164] M.D.C. Giménez-López, F. Moro, A. La Torre, C.J. Gómez-García, P.D. Brown, J. van Slageren, A.N. Khlobystov, Encapsulation of single-molecule magnets in carbon nanotubes, Nat. Commun. 2 (Jan. 2011) 407.
[165] F. Simon, H. Kuzmany, H. Rauf, T. Pichler, J. Bernardi, H. Peterlik, L. Korecz, F. Fülöp, A. Jánossy, Low temperature fullerene encapsulation in single wall carbon nanotubes: synthesis of N@C60@SWCNT, Chem. Phys. Lett. 383 (Jan. 2004) 362–367.
[166] G. Pagona, G. Rotas, A.N. Khlobystov, T.W. Chamberlain, K. Porfyrakis, N. Tagmatarchis, Azafullerenes encapsulated within single-walled carbon nano-tubes, J. Am. Chem. Soc. 130 (May 2008) 6062–6063.
[167] D.A. Britz, A.N. Khlobystov, K. Porfyrakis, A. Ardavan, G.A.D. Briggs, Chemical reactions inside single-walled carbon nano test-tubes, in: Chemical Communications, Cambridge, England, Jan. 2005, pp. 37–39.
[168] R. Pfeiffer, M. Holzweber, H. Peterlik, H. Kuzmany, Z. Liu, K. Suenaga, H. Kataura, Dynamics of carbon nanotube growth from fullerenes, Nano Lett. 7 (Aug. 2007) 2428–2434.
[169] H. Shiozawa, T. Pichler, A. Grüneis, R. Pfeiffer, H. Kuzmany, Z. Liu, K. Suenaga, H. Kataura, A catalytic reaction inside a single-walled carbon nanotube, Adv. Mater. 20 (Apr. 2008) 1443–1449.
[170] T.W. Chamberlain, J.C. Meyer, J. Biskupek, J. Leschner, A. Santana, N.A. Besley, E. Bichoutskaia, U. Kaiser, A.N. Khlobystov, Reactions of the inner surface of carbon nanotubes and nanoprotrusion processes imaged at the atomic scale, Nat. Chem. 3 (Aug. 2011) 732–737.
[171] A. Chuvilin, A.N. Khlobystov, D. Obergfell, M. Haluska, S. Yang, S. Roth, U. Kaiser, Observations of chemical reactions at the atomic scale: dynamics of metal-mediated fullerene coalescence and nanotube rupture, Angew. Chem., Int. Ed. Engl. 49 (Jan. 2010) 193–196.
[172] W. Plank, R. Pfeiffer, C. Schaman, H. Kuzmany, M. Calvaresi, F. Zerbetto, J. Meyer, Electronic structure of carbon nanotubes with ultrahigh curvature, ACS Nano 4 (Aug. 2010) 4515–4522.
[173] C. Guerret-Piécourt, Y.L. Bouar, A. Loiseau, H. Pascard, Relation between metal electronic structure and morphology of metal compounds inside carbon nanotubes, Nature 372 (Dec. 1994) 761–765.
[174] R.R. Meyer, J. Sloan, R.E. Dunin-Burkowski, A.I. Kirkland, M.C. Novotny, S.R. Bailey, J.L. Hutchison, M.L.H. Green, Discrete atom imaging of one-dimensional crystals formed within single-walled carbon nanotubes, Science 289 (Aug. 2000) 1324–1326.
[175] J. Sloan, A. Kirkland, J. Hutchison, Structural characterization of atomically regulated nanocrystals formed within single-walled carbon nanotubes using electron microscopy, Acc. Chem. Res. 35 (12) (2002) 1054–1062.
[176] K. Kobayashi, K. Suenaga, T. Saito, S. Iijima, Prevention of Sn and Pb crystallization in a confined nanospace, Small 6 (June 2010) 1279–1282 (Weinheim an der Bergstrasse, Germany).
[177] A. Chuvilin, E. Bichoutskaia, M.C. Gimenez-Lopez, T.W. Chamberlain, G.A. Rance, N. Kuganathan, J. Biskupek, U. Kaiser, A.N. Khlobystov, Self-assembly of a sulphur-terminated graphene nanoribbon within a single-walled carbon nanotube, Nat. Mater. 10 (Sept. 2011) 687–692.
[178] X. Zhao, Y. Ando, Y. Liu, M. Jinno, T. Suzuki, Carbon nanowire made of a long linear carbon chain inserted inside a multiwalled carbon nanotube, Phys. Rev. Lett. 90 (May 2003) 187401.
[179] J. Hu, Y. Bando, J. Zhan, C. Zhi, D. Golberg, Carbon nanotubes as nanoreactors for fabrication of single-crystalline Mg3N2 nanowires, Nano Lett. 6 (June 2006) 1136–1140.
[180] M. Koshino, T. Tanaka, N. Solin, K. Suenaga, H. Isobe, E. Nakamura, Imaging of single organic molecules in motion, Science 316 (May 2007) 853.
[181] R. Erni, M. Rossell, M.-T. Nguyen, S. Blankenburg, D. Passerone, P. Hartel, N. Alem, K. Erickson, W. Gannett, A. Zettl, Stability and dynamics of small molecules trapped on graphene, Phys. Rev. B 82 (Oct. 2010) 1–6.
[182] F. Schäffel, M. Wilson, J.H. Warner, Motion of light adatoms and molecules on the surface of few-layer graphene, ACS Nano (Nov. 2011).
[183] R.S. Pantelic, J.C. Meyer, U. Kaiser, H. Stahlberg, The application of graphene as a sample support in transmission electron microscopy, Solid State Commun. 152 (Apr. 2012) 1375–1382.
[184] W. Zhou, S.J. Pennycook, J.-C. Idrobo, Probing the electronic structure and optical response of a graphene quantum disk supported on monolayer graphene, J. Phys. Condens. Matter 24 (Aug. 2012) 314213.
[185] P.Y. Huang, S. Kurasch, A. Srivastava, V. Skakalova, J. Kotakoski, A.V. Krasheninnikov, R. Hovden, Q. Mao, J.C. Meyer, J. Smet, D.A. Muller, U. Kaiser, Direct imaging of a two-dimensional silica glass on graphene, Nano Lett. 12 (Feb. 2012) 1081–1086.

[186] Z. Lee, K.-J. Jeon, A. Dato, R. Erni, T.J. Richardson, M. Frenklach, V. Radmilovic, Direct imaging of soft-hard interfaces enabled by graphene, Nano Lett. 9 (Sept. 2009) 3365–3369.
[187] N.R. Wilson, P.A. Pandey, R. Beanland, R.J. Young, I.A. Kinloch, L. Gong, Z. Liu, K. Suenaga, J.P. Rourke, S.J. York, J. Sloan, Graphene oxide: structural analysis and application as a highly transparent support for electron microscopy, ACS Nano 3 (Sept. 2009) 2547–2556.
[188] J.H. Warner, M.H. Rümmeli, A. Bachmatiuk, M. Wilson, B. Büchner, Examining co-based nanocrystals on graphene using low-voltage aberration-corrected transmission electron microscopy, ACS Nano 4 (Jan. 2010) 470–476.
[189] R.R. Nair, P. Blake, J.R. Blake, R. Zan, S. Anissimova, U. Bangert, A.P. Golovanov, S.V. Morozov, A.K. Geim, K.S. Novoselov, T. Latychevskaia, Graphene as a transparent conductive support for studying biological molecules by transmission electron microscopy, Appl. Phys. Lett. 97 (Oct. 2010) 153102.
[190] R.S. Pantelic, J.C. Meyer, U. Kaiser, W. Baumeister, J.M. Plitzko, Graphene oxide: a substrate for optimizing preparations of frozen-hydrated samples, J. Struct. Biol. 170 (Apr. 2010) 152–156.
[191] R.S. Pantelic, J.W. Suk, C.W. Magnuson, J.C. Meyer, P. Wachsmuth, U. Kaiser, R.S. Ruoff, H. Stahlberg, Graphene: Substrate preparation and introduction, J. Struct. Biol. 174 (Apr. 2011) 234–238.
[192] R.S. Pantelic, J.W. Suk, Y. Hao, R.S. Ruoff, H. Stahlberg, Oxidative doping renders graphene hydrophilic, facilitating its use as a support in biological TEM, Nano Lett. 11 (Oct. 2011) 4319–4323.
[193] D. Rhinow, M. Bueenfeld, N.-E. Weber, A. Beyer, A. Goelzhaeuser, W. Kuehlbrandt, N. Hampp, A. Turchanin, Energy-filtered transmission electron microscopy of biological samples on highly transparent carbon nanomembranes, Ultramicroscopy 111 (5) (2011) 342–349.
[194] D. Rhinow, N.-E. Weber, A. Turchanin, A. Gölzhäuser, W. Kühlbrandt, Single-walled carbon nanotubes and nanocrystalline graphene reduce beam-induced movements in high-resolution electron cryo-microscopy of ice-embedded biological samples, Appl. Phys. Lett. 99 (13) (2011) 133701.
[195] M.A. Dyson, A.M. Sanchez, J.P. Patterson, R.K. O'Reilly, J. Sloan, N.R. Wilson, A new approach to high resolution, high contrast electron microscopy of macromolecular block copolymer assemblies, Soft Matter 9 (14) (2013) 3741.
[196] J. Jeon, M.S. Lodge, B.D. Dawson, M. Ishigami, F. Shewmaker, B. Chen, Superb resolution and contrast of transmission electron microscopy images of unstained biological samples on graphene-coated grids, Biochim. Biophys. Acta 1830 (June 2013) 3807–3815.
[197] B. Westenfelder, J.C. Meyer, J. Biskupek, S. Kurasch, F. Scholz, C.E. Krill, U. Kaiser, Transformations of carbon adsorbates on graphene substrates under extreme heat, Nano Lett. 11 (Oct. 2011) 5123–5127.
[198] K. Kim, W. Regan, B. Geng, B. Alemán, B.M. Kessler, F. Wang, M.F. Crommie, A. Zettl, High-temperature stability of suspended single-layer graphene, Phys. Status Solidi RRL 4 (Nov. 2010) 302–304.
[199] A. Chuvilin, U. Kaiser, E. Bichoutskaia, N.A. Besley, A.N. Khlobystov, Direct transformation of graphene to fullerene, Nat. Chem. 2 (May 2010) 450–453.
[200] N. Mohanty, M. Fahrenholtz, A. Nagaraja, D. Boyle, V. Berry, Impermeable graphenic encasement of bacteria, Nano Lett. 11 (Mar. 2011) 1270–1275.
[201] M. Krueger, S. Berg, D. Stone, E. Strelcov, D.A. Dikin, J. Kim, L.J. Cote, J. Huang, A. Kolmakov, Drop-casted self-assembling graphene oxide membranes for scanning electron microscopy on wet and dense gaseous samples, ACS Nano 5 (Nov. 2011) 10047–10054.
[202] J.M. Yuk, J. Park, P. Ercius, K. Kim, D.J. Hellebusch, M.F. Crommie, J.Y. Lee, A. Zettl, A.P. Alivisatos, High-resolution EM of colloidal nanocrystal growth using graphene liquid cells, Science 336 (Apr. 2012) 61–64.
[203] A.K. Geim, K.S. Novoselov, The rise of graphene, Nat. Mater. 6 (Mar. 2007) 183–191.
[204] P.Y. Huang, J.C. Meyer, D.A. Muller, From atoms to grains: Transmission electron microscopy of graphene, Mater. Res. Soc. Bull. 37 (Nov. 2012) 1214–1221.
[205] B.I. Yakobson, F. Ding, Observational geology of graphene, at the nanoscale, ACS Nano 5 (Mar. 2011) 1569–1574.
[206] L.P. Biró, P. Lambin, Grain boundaries in graphene grown by chemical vapor deposition, New J. Phys. 15 (Mar. 2013) 035024.
[207] D. Van Dyck, J.R. Jinschek, F.-R. Chen, Big Bang tomography as a new route to atomic-resolution electron tomography, Nature 486 (June 2012) 243–246.
[208] K.S. Novoselov, V.I. Falko, L. Colombo, P.R. Gellert, M.G. Schwab, K. Kim, A roadmap for graphene, Nature 490 (Oct. 2012) 192–200.
[209] K.S. Novoselov, D. Jiang, F. Schedin, T.J. Booth, V.V. Khotkevich, S.V. Morozov, A.K. Geim, Two-dimensional atomic crystals, Proc. Natl. Acad. Sci. USA 102 (30) (2005) 10451–10453.
[210] J.C. Meyer, A. Chuvilin, G. Algara-Siller, J. Biskupek, U. Kaiser, Selective sputtering and atomic resolution imaging of atomically thin boron nitride membranes, Nano Lett. 9 (July 2009) 2683–2689.
[211] C. Jin, F. Lin, K. Suenaga, S. Iijima, Fabrication of a freestanding boron nitride single layer and its defect assignments, Phys. Rev. Lett. 102 (May 2009) 3–6.
[212] J.N. Coleman, M. Lotya, A. O'Neill, S.D. Bergin, P.J. King, U. Khan, K. Young, A. Gaucher, S. De, R.J. Smith, I.V. Shvets, S.K. Arora, G. Stanton, H.-Y. Kim, K. Lee, G.T. Kim, G.S. Duesberg, T. Hallam, J.J. Boland, J.J. Wang, J.F. Donegan, J.C. Grunlan, G. Moriarty, A. Shmeliov, R.J. Nicholls, J.M. Perkins, E.M. Grieveson, K. Theuwissen, D.W. McComb, P.D. Nellist, V. Nicolosi, Two-dimensional nanosheets produced by liquid exfoliation of layered materials, Science (New York, NY) 331 (Feb. 2011) 568–571.
[213] H.-P. Komsa, J. Kotakoski, S. Kurasch, O. Lehtinen, U. Kaiser, A. Krasheninnikov, Two-dimensional transition metal dichalcogenides under electron irradiation: defect production and doping, Phys. Rev. Lett. 109 (July 2012) 035503.